

Cenozoic tectonic evolution of Qaidam basin and its surrounding regions (Part 1): The southern Qilian Shan-Nan Shan thrust belt and northern Qaidam basin

An Yin

Structural Geology Group, School of Earth Sciences and Resources, China University of Geosciences, Beijing 100083, China
Permanent address: Department of Earth and Space Sciences and Institute of Geophysics and Planetary Physics, University of California, Los Angeles, California 90095-1567, USA

Yu-Qi Dang

Li-Cun Wang

Wu-Ming Jiang

Su-Ping Zhou

Qinghai Oilfield Company, Dunhuang 736202, Gansu Province, People's Republic of China

Xuan-Hua Chen

Institute of Geomechanics, Chinese Academy of Geological Sciences, Beijing 100081, People's Republic of China

George E. Gehrels

Department of Geosciences, University of Arizona, Tucson, Arizona 85721-0071

Michael W. McRivette

Department of Earth and Space Sciences and Institute of Geophysics and Planetary Physics, University of California, Los Angeles, California 90095-1567, USA

ABSTRACT

Cenozoic Qaidam basin, the largest active intermountain basin inside Tibet, figures importantly in the debates on the history and mechanism of Tibetan plateau formation during the Cenozoic Indo-Asian collision. To determine when and how the basin was developed, we conducted detailed geologic mapping and analyses of a dense network of seismic reflection profiles from the southern Qilian Shan-Nan Shan thrust belt and northern Qaidam basin. Our geologic observations provide new constraints on the timing and magnitude of Cenozoic crustal thickening in northern Tibet. Specifically, our work shows that the southernmost part of the Qilian Shan-Nan Shan thrust belt and contractional structures along the northern margin of Qaidam basin were initiated in the Paleocene-early Eocene (65–50 Ma), during or immediately after the onset of the Indo-Asian collision. This finding implies that stress was transferred rapidly through Tibetan

lithosphere to northern Tibet from the Indo-Asian convergent front located >1000 km to the south. The development of the thrust system in northern Qaidam basin was driven by motion on the Altyn Tagh fault, as indicated by its eastward propagation away from the Altyn Tagh fault. The eastward lengthening of the thrust system was spatially and temporally associated with eastward expansion of Qaidam basin, suggesting thrust loading was the main control on the basin formation and evolution. The dominant structure in northern Qaidam basin is a southwest-tapering triangle zone, which started to develop since the Paleocene and early Eocene (65–50 Ma) and was associated with deposition of an overlying southwest-thickening, growth-strata sequence. Recognition of the triangle zone and its longevity in northern Qaidam basin explains a long puzzling observation that Cenozoic depocenters have been located consistently along the central axis of the basin. This basin configuration is opposite to the prediction of classic foreland-basin models that require the thickest part of foreland sediments deposited along basin

edges against basin-bounding thrusts. Restoration of balanced cross sections across the southern Qilian Shan-Nan Shan thrust belt and northern Qaidam basin suggests that Cenozoic shortening strain is highly inhomogeneous, varying from ~20% to >60%, both vertically in a single section and from section to section across the thrust belt. The spatially variable strain helps explain the conflicting paleomagnetic results indicating different amounts of Cenozoic rotations in different parts of Qaidam basin. The observed crustal shortening strain also implies that no lower-crustal injection or thermal events in the mantle are needed to explain the current elevation (~3000–3500 m) and crustal thickness (45–50 km) of northern Qaidam basin and the southern Qilian Shan-Nan Shan thrust belt. Instead, thrusting involving continental crystalline basement has been the main mechanism of plateau construction across northern Qaidam basin and the southern Qilian Shan-Nan Shan region.

Keywords: Tibetan plateau, Qaidam basin, Qilian Shan, Nan Shan, thrust tectonics.

E-mail: yin@ess.ucla.edu

INTRODUCTION

Understanding the evolution of the Tibetan plateau has two fundamental implications in Earth sciences. First, its growth mechanism provides a key constraint on the dynamics of large-scale continental deformation (e.g., England and Houseman, 1986; Tapponnier et al., 1982, 2001). Second, its growth history provides an observational basis for quantifying feedback processes between lithospheric deformation, atmospheric circulation, and biological evolution (Harrison et al., 1992; Molnar et al., 1993). Despite these important implications, no consensus has been reached on the plateau-forming mechanisms. Hypotheses vary from uniform lithospheric shortening, thrust imbrications in the upper crust and mantle lithosphere associated with flow in the lower crust, lower-crustal injection and lateral flow, continental subduction, convective removal of mantle lithosphere, to large-scale underthrusting (e.g., Zhao and Morgan, 1985, 1987; England and Houseman, 1986; Dewey et al., 1988; England and Houseman, 1989; Burg et al., 1994; Royden, 1996; Clark and Royden, 2000; Owens and Zandt, 1997; Tapponnier et al., 2001; DeCelles et al., 2002). Similarly, there is little agreement on the formation history of the Tibetan plateau. In one view, the plateau has grown progressively from south to north and the northward-marching deformation front did not reach the present Qilian Shan-Nan Shan region of northern Tibet until 15–5 Ma (e.g., Molnar and Tapponnier, 1975; Burchfiel and Royden, 1991; Métivier et al., 1998). In a contrasting view, deformation induced by the Indo-Asian collision may have occurred across the present extent of the Tibetan plateau at ca. 50 Ma during or soon after the onset of the Indo-Asian collision (Burg et al., 1994; Yin et al., 2002).

The competing views on the formation history of the Tibetan plateau have different implications for the plateau-growth mechanisms. For those who advocate a progressive northward growth of Tibet, the plateau may have been enlarged either in a continuous manner (England and Houseman, 1986; also see Burchfiel and Royden, 1991) or in discrete fashion via a stepwise jumping of the northern plateau margin (Meyer et al., 1998; Métivier et al., 1998). The continuous-growth model implies the continental lithosphere to behave as a viscous fluid, while the stepwise-jump model requires continental lithosphere to deform as a strain-softening material capable of localizing and maintaining motion on continental-scale faults for tens of millions of years. Coeval initiation of deformation in present northern Tibet and the onset of the Indo-Asian collision (Yin et al., 2002) implies that the preexisting weakness of the Tibetan pla-

teau and buckling instability of a strong Tibetan lithosphere may have played an important role in controlling the spatial and temporal evolution of the plateau (e.g., Burg et al., 1994; Kong et al., 1997; Yin and Harrison, 2000).

Qaidam basin is the largest active intermountain basin inside Tibet (Fig. 1) and figures importantly in the debate on the development of the Tibetan plateau. In the classic treatise on the Chinese sedimentary basins, Bally et al. (1986) propose the basin to have formed in the core of a large synclorium between two thrust belts across the Qilian Shan in the north and the Eastern Kunlun Shan in the south. Expanding on this view, Yin et al. (2002) propose that Qaidam basin initiated in the middle Eocene and formed as a common foreland basin between a southwest-directed thrust system in the north (Qilian Shan-Nan Shan thrust belt) and a northeast-directed thrust system in the south (Qimen Tagh-Eastern Kunlun thrust belt) (Fig. 1A). Yin et al. (2002) also considered the western basin boundary to have been progressively closed by southwest motion of the Altyn Tagh Range along the Altyn Tagh fault, causing Qaidam to become an internally drained basin since the early Oligocene (i.e., the sliding door model). Burchfiel et al. (1989) postulate a basement-involved thrust belt across the basin, which is linked with the Qilian Shan-Nan Shan thrust belt by a northeast-directed detachment fault in the middle crust. In contrast to the above view, Meyer et al. (1998) and Métivier et al. (1998) suggest that the Qaidam basin may have been trapped in the middle Miocene to Pliocene as a result of northward jumping of the deformation front from the Eastern Kunlun Range to the Qilian Shan-Nan Shan region across the basin. More recently, Wang et al. (2006) postulate the presence of an Oligocene-Pliocene longitudinal river sourced in the Pamirs region with its eastern termination migrating progressively eastward across Qaidam basin during eastward extrusion of the northern Tibetan plateau.

To test the various hypotheses on the tectonic development of Qaidam basin, we conducted detailed field mapping in the southern Qilian Shan and Nan Shan thrust belt and performed a systematic analysis of a dense network of seismic-reflection profiles and drill-hole data across northern Qaidam basin. The results presented in this paper represent the first of a three-part series on the Cenozoic evolution of Qaidam basin: the second part deals with the evolution of the southern margin of Qaidam basin and the Qimen Tagh-Eastern Kunlun thrust belt (Yin et al., 2007), while the third part deals with the Cenozoic history of the whole Qaidam basin (Yin et al., 2007). The observations presented in this paper have three important implications

for the formation history and growth mechanism of the Tibetan plateau. First, they suggest that Cenozoic contractional deformation in northern Tibet started in the Paleocene and early Eocene (65–50 Ma) during or immediately after the onset of the Indo-Asian collision. Second, the magnitude of Cenozoic crustal shortening strain across the region is sufficient to explain its current elevation and crustal thickness without invoking lower crustal flow and a thermal event in the mantle. Third, the sedimentary architecture of Qaidam basin, characterized by its depocenters persistently located along the basin axis, was created by the development of crustal-scale triangle zones tapering from the basin margins toward the basin interior (also see Yin et al. [2007] for the structural evolution of the southern margin of Qaidam basin).

GEOLOGY OF THE Q Aidam BASIN

With an average elevation of ~2800 m, Qaidam basin is triangular in map view, bounded by the Altyn Tagh fault in the northwest, the Qilian Shan-Nan Shan thrust belt in the northeast, and the Eastern Kunlun transpressional system (including the Qimen Tagh-Eastern Kunlun thrust belt and the Kunlun fault) in the south (Fig. 1A). Although the crustal thickness of Qaidam basin is ~10–25 km thinner than its surrounding mountain ranges at ~45–50 km (Zhu and Helmberger, 1998; Zhao et al., 2006; Li, S.L., et al., 2006; Li, Y.H., et al., 2006), its effective elastic thickness (T_e) is ~70 km, which is significantly greater than the values of 10–30 km for the rest of the Tibetan plateau (Braitenberg et al., 2003).

Cenozoic deformation across Qaidam basin has mostly been investigated by paleomagnetic studies and interpretations of subsurface data (seismic profiles and drill-hole data thanks to 50 years of petroleum exploration across the region) (Sun and Sun, 1959; Huang et al., 1996; Dang et al., 2003). From the studies on Cretaceous and Cenozoic samples along the Altyn Tagh fault and northern Qaidam basin, Dupont-Nivet et al. (2002) and Sun et al. (2006) concluded that no Cenozoic rotation has occurred for the whole Qaidam block. In contrast, paleomagnetic studies of Jurassic to Neogene strata in northern and southwestern Qaidam led Chen et al. (2002) and Halim et al. (2003) to infer that Qaidam basin has rotated clockwise 16–20°. Although the above conflicting paleomagnetic results could be reconciled by inhomogeneous Cenozoic deformation across the basin, because the samples of each study came from different parts of the basin, no systematic structural studies have been conducted to test this possibility. Bally et al. (1986) used seismic data to show the presence of middle Eocene growth strata against

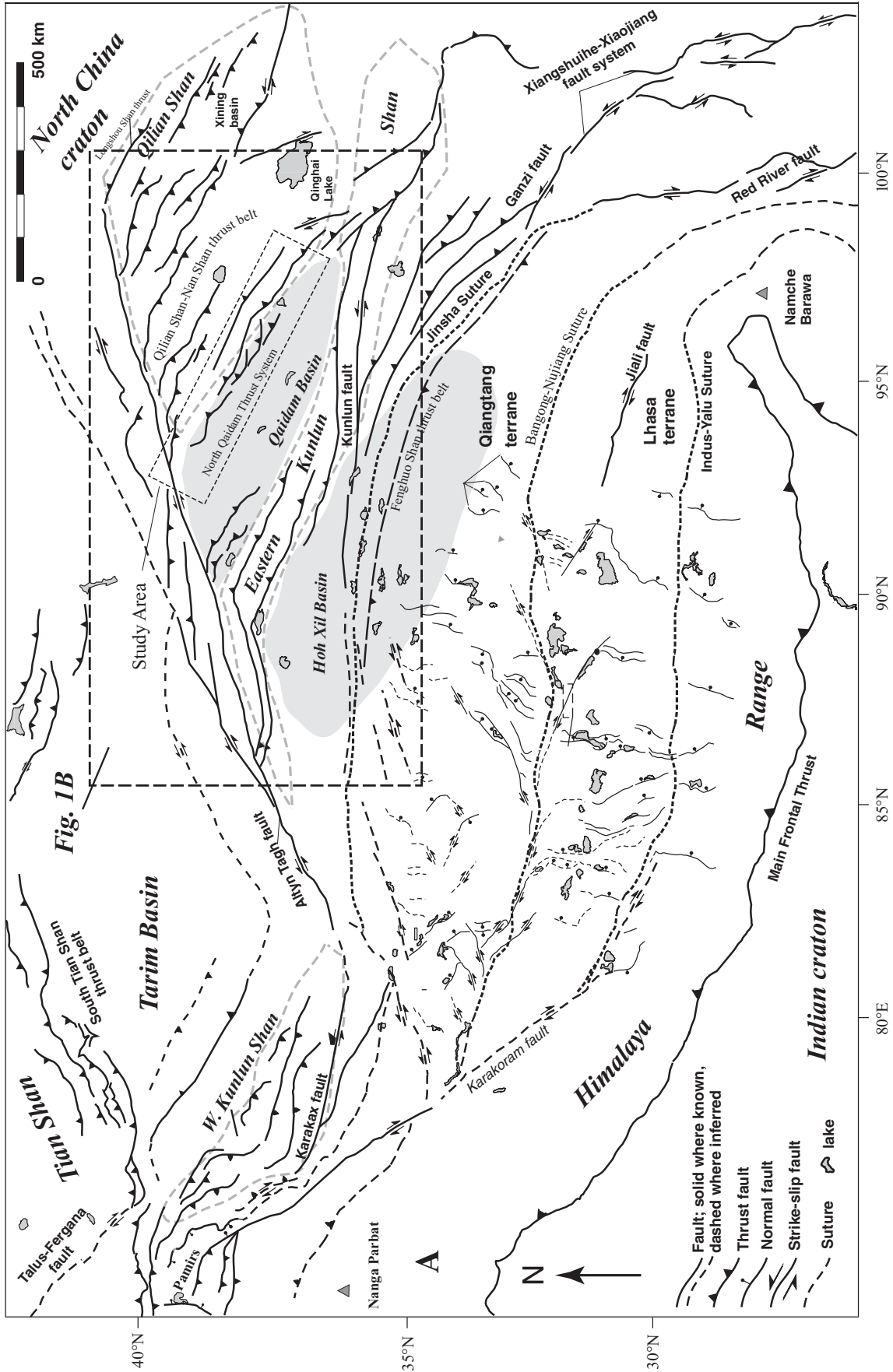


Figure 1. (A) Cenozoic tectonic map of the Tibetan plateau and the location of the North Qaidam thrust system. The figure is modified from Taylor et al. (2003). (B) Tectonic map of the central and northern Tibetan plateau. The North Qaidam thrust system is located in the southern Qilian Shan-Shan thrust belt and bounds the northern margin of the Qaidam basin. Major contractional structures in the North Qaidam thrust system are also indicated: (1) Dasaibei thrust (DS), (2) Xiaosaibei thrust (XS), (3) Sainan thrust (SN), (4) Qaidam thrust (QD), (5) Western Luliang thrust (WL), (6) Eastern Luliang thrust (EL), (7) Xitfe Shan thrust (XT), (8) the Olongbulak thrust (OL), (9) Ainunuk thrust (AM), (10) the Changshan anticline (CSA), and (11) the Dalang anticline (DLA). The eastern margin of Qaidam basin at the end of the Paleocene to early Eocene (E1+2), Middle Eocene to early Oligocene (E3), late Oligocene (N1), and late Miocene (N2-2) and are also shown. (Continued on following page.)

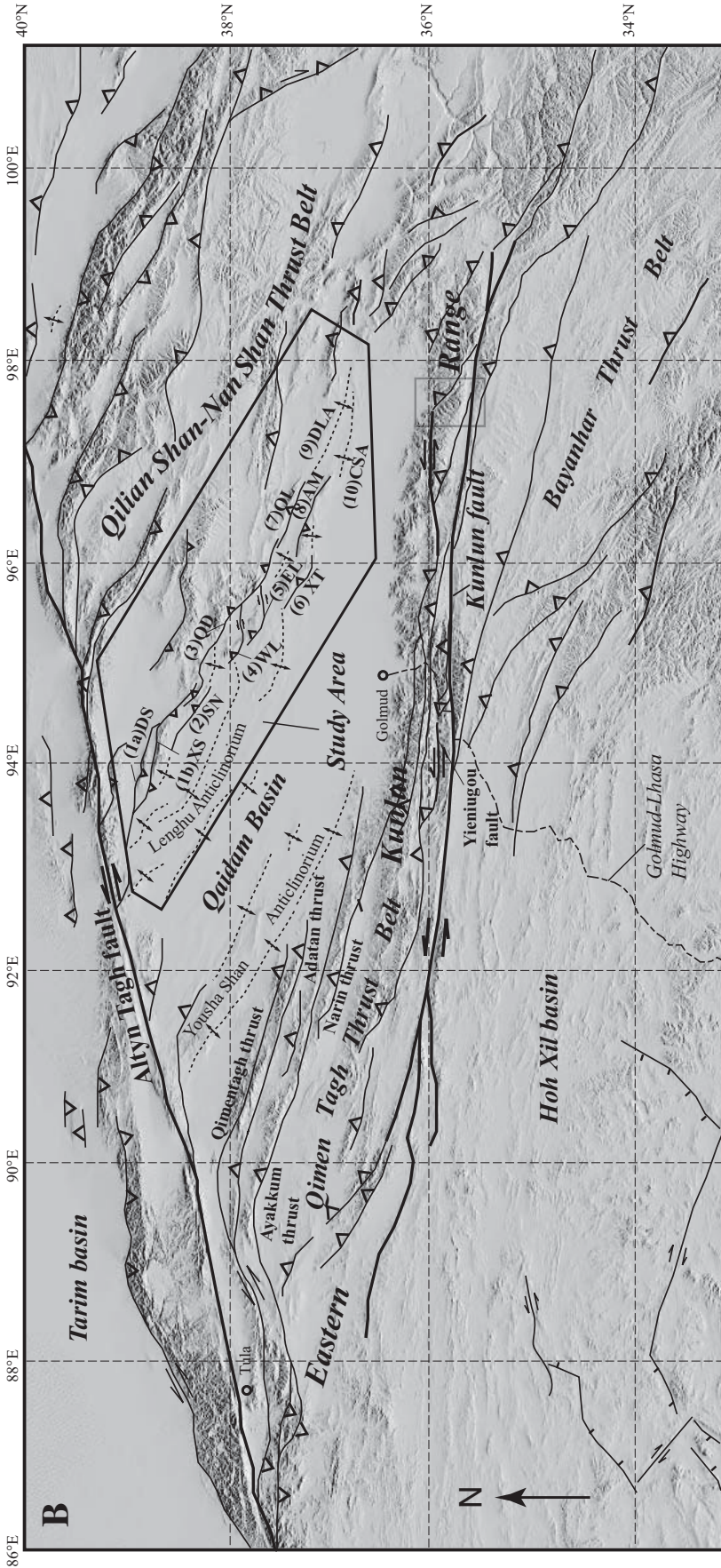


Figure 1 (continued).

the Altyin Tagh fault along the western edge of Qaidam basin and interpreted this observation as indicating the Altyin Tagh fault to have initiated at this time. Using both drill-hole and seismic data in southwestern Qaidam, Song and Wang (1993) infer a major south-dipping thrust along the southern margin of Qaidam basin. Huang et al. (1996) and Zhou et al. (2006) provide the most complete structural synthesis of the whole Qaidam basin with emphasis on high-angle thrusting that requires minimal horizontal shortening across the basin (<10 km).

Qaidam basin preserves a complete record of Cenozoic sedimentation and has been the focus of numerous studies (Bally et al., 1986; Wang and Coward, 1990; Song and Wang, 1993; Huang et al., 1996; Zhang, 1997; Métiévier et al., 1998; Xia et al., 2001; Yin et al., 2002; Dang et al., 2003; Sobel et al., 2003; Sun et al., 2005; Rieser et al., 2005, 2006a, 2006b; Zhou et al., 2006). For example, sedimentological development of the basin has been established by analyzing thickness distribution (Huang et al., 1996), paleocurrent directions (Hanson, 1998), lithofacies patterns (e.g., Zhang, 1997), sandstone petrology (Rieser et al., 2005), and ⁴⁰Ar/³⁹Ar ages of detrital micas (Rieser et al., 2006a, 2006b). These studies suggest that the Cenozoic Qaidam basin has expanded progressively eastward since the initiation of the basin in the Paleocene-early Eocene, with its depocenters consistently located along the axis of the basin. These observations have led Wang et al. (2006) to propose the presence of a paleo-longitudinal river flowing eastward along the axis of Qaidam basin.

Cenozoic stratigraphic division and age assignments across Qaidam basin are based on outcrop geology and its correlation with subsurface data (seismic reflection profiles and drill-hole data), terrestrial fossils (i.e., spores, ostracods, and pollen), basin-wide stratigraphic correlation via a dense network of seismic reflection profiles, magnetostratigraphic studies, and fission-track and ⁴⁰Ar/³⁹Ar dating of detrital micas (Huo, 1990; Qinghai Bureau of Geology and Mineral Resources [BGMR], 1991; Yang et al., 1992; Song and Wang, 1993; Huang et al., 1996; Xia et al., 2001; Nansheng, 2002; Sun et al., 2005; Rieser et al., 2006a, 2006b). Major Cenozoic stratigraphic units in Qaidam basin include (Table 1): the Paleocene to early Eocene Lulehe Formation (E1+2; 65–49 Ma) (Yang, 1988; Huo, 1990; Yang et al., 1992; Rieser et al., 2006a, 2006b), the middle and late Eocene Lower Xiangancaigou Formation (E3–1; 49–37 Ma) (Yang et al., 1992; Sun et al., 2005), the early Oligocene Upper Xiangancaigou Formation (E3–2; 37–28.5 Ma) (Sun et al., 1999), the late Oligocene Shanggancaigou Formation

TABLE 1. MESOZOIC AND CENOZOIC STRATIGRAPHY OF Q Aidam Basin

Unit names	Symbol	Geologic time	Age (Ma)
Dabuxun Yanqiao Formation	Q2	Holocene	0.01 Ma–present
Qigequan Formation	Q1	Pleistocene	1.8–0.01
Shizigou Formation	N2-3	Pliocene	5.3–1.8
Shangyoushashan Formation	N2-2	late Miocene	11.2–5.3
Xiayoushashan Formation	N2-1	early and middle Miocene	23.8–11.2
Shangganchaigou Formation	N1	late Oligocene	28.5–23.8
Upper Xiaganchaigou Formation	E3-2	early Oligocene	37–28.5
Lower Xiaganchaigou Formation	E3-1	middle Eocene–late Eocene	49–37
Lulehe Formation	E1+2	Paleocene–Early Eocene	>54.8–49
(Jurassic strata, locally overlain by Cretaceous beds)	Jr	Jurassic-Cretaceous	206–65

(N1; 28.5–23.8 Ma) (Sun et al., 1999), the early to middle Miocene Xiayoushashan Formation (N2–1; 23.5–11.2 Ma) (Sun et al., 1999), the late Miocene Shangyoushashan Formation (N2–2; 11.2–5.3 Ma) (Sun et al., 1999), the Pliocene Shizigou Formation (N2–3; 5.3–1.8 Ma) (Sun et al., 1999), the Pleistocene Qigequan Formation (Q1; 1.8–0.01 Ma) (Sun et al., 1999), and the Holocene Dabuxun Yanqiao Formation (Q2) (Yang et al., 1997). Our age division closely follows that of Rieser et al. (2006a, 2006b) and Sun et al. (2005).

STRUCTURAL GEOLOGY OF NORTH Q Aidam THRUST SYSTEM

Surface Geology

The 500-km-long North Qaidam thrust system is located in the southernmost part of the Cenozoic Qilian Shan-Nan Shan thrust belt (Fig. 1B). It consists of the following major structures: (1) the northeast-directed Saishiteng thrust zone that includes the northeast-directed Dasaibei thrust (DS) in the north and the northeast-directed Xiaosaibei thrust (XS) in the south; (2) the southwest-directed Sainan thrust zone (SN) that lies south of the Saishiteng thrust zone and dies out laterally into northwest-trending anticlines; (3) the southwest-directed Qaidam Shan thrust zone (QD) terminating in the west in the Xiaosaibei-thrust hanging wall and in the east in an anticline; (4) the L-shaped and southwest-directed Western and Eastern Luliang thrusts (WL and EL) that merge separately northward with the overriding Qaidam Shan thrust zone; (5) the southwest-directed Xitie Shan thrust zone (XT) that lies south of the Qaidam Shan thrust zone and dies out laterally into folds; (6) the southwest-directed Olongbulak thrust zone (OL) that terminates in the footwall of the Qaidam Shan thrust zone in the west and the Dalang anticline (DLA) in the east; (7) the northeast-directed Aimunik thrust zone (AM) that lies directly south of the Olongbulak thrust zone and dies out eastward into the

Changshan anticline (CSA); and (8) the Lenghu anticlinorium consisting of a series of folds and lying directly south of the Saishiteng and Sainan thrust zones. Before describing each structure in the North Qaidam thrust system, we briefly summarize the pre-Cenozoic deformation history of the North Qaidam region.

The Cenozoic Qilian Shan-Nan Shan thrust belt was a locus of intense early Paleozoic deformation induced by a series of arc-arc and arc-continent collisional events (Li et al., 1978; Yin and Nie, 1996; Yin and Harrison, 2000; Yang et al., 2001; Gehrels et al., 2003a, 2003b). The area also experienced widespread Mesozoic extension as expressed by the development of Jurassic and Cretaceous extensional basins (e.g., Huo and Tan, 1995; Vincent and Allen, 1999; Xia et al., 2001; Dang et al., 2003; Horton et al., 2004; cf. Ritts and Biffi, 2000), Jurassic and Cretaceous detachment faulting that had induced rapid cooling in the detachment footwalls and growth strata in the hanging-wall half grabens (Chen et al., 2003), and Jurassic basaltic eruptions (Guo et al., 1999). The southernmost part of the thrust belt against Qaidam basin, where this study was conducted, exposes Precambrian gneisses, early Paleozoic ultrahigh-pressure metamorphic rocks, and metamorphosed Ordovician-Silurian arc sequences (e.g., Yang et al., 2001; Zhang et al., 2005; Song et al., 2005; Yin et al., 2008a). The metamorphic rocks are overlain unconformably by unmetamorphosed Devonian to Cenozoic marine and continental strata (Liu, 1988; Qinghai BGMR, 1991; Yang et al., 2001). Pre-Devonian structures are mainly isoclinal folds associated with development of ductile fabrics such as cleavage, gneissic foliation, and ductile shear zones (Yang et al., 2001; Yin et al., 2008a) (Figs. 2 and 6). Although early Paleozoic ductile structures can be easily differentiated from Cenozoic brittle structures, contractional deformation in unmetamorphosed Devonian to Cretaceous rocks and Cenozoic strata shares a similar style. For this reason, our mapping focuses mainly on areas exposing Cenozoic strata.

Accurate construction of geologic cross sections requires the portrayed style of deformation to be consistent with that observed in the field. As shown below, map patterns, direct field observations, and structures imaged in seismic reflection profiles all indicate that folds across northern Qaidam basin exhibit rather broad and round, fold hinge-zone geometry. To simulate this folding style, we first establish the general structural framework using the dip-domain method to honor all the measured bedding attitudes at surface (Suppe, 1983; Suppe and Medwedeff, 1990). We then use a round fold-hinge geometry to smooth the artificially created kinks so that the fold style in the cross sections matches those observed in the field and seismic reflection profiles. This hybrid method produces broader fold-hinge zones and smaller fold amplitudes than those created solely by the kink-bend method and matches well the drill-hole data that constrain the depth distribution of fold limbs and fold hinge zones.

The geometric and kinematic plausibility of each cross section (including those constructed from seismic profiles) was verified by a step-by-step palinspastic restoration. The restoration was conducted by removing sequentially the effect of deformation and associated sedimentation from the youngest to oldest deformation event. Strain compatibility of neighboring restored panels sharing a common geologic contact was achieved by bedding-parallel shear after all the beds in the panels were laid down horizontally. The success of this simple procedure in restoring all the sections suggests that inter-bedding flexural slip is the main folding mechanism to have accommodated Cenozoic deformation.

The restored sections allow us to estimate the total amount of shortening and the associated shortening strain by comparing the present and restored lengths of the cross sections. As in all the restored sections, different beds may have different amounts of shortening as induced by (1) the presence of bedding-parallel faults, (2) development of growth strata with the younger synkinematic units only recording a fraction of the total Cenozoic strain, and (3) erosion causing partial removal of some stratigraphic units in the sections. To avoid the above complications, we chose our reference unit with the following two criteria: (1) it has the most complete bed length in the section, and (2) it was deposited immediately prior to the onset of Cenozoic deformation. These criteria led us to use mostly the Jurassic-Cretaceous beds as the reference horizon to calculate horizontal shortening.

Saishiteng Thrust Zone

The Saishiteng thrust zone consists of the northeast-directed Dasaibei and Xiaosaibei

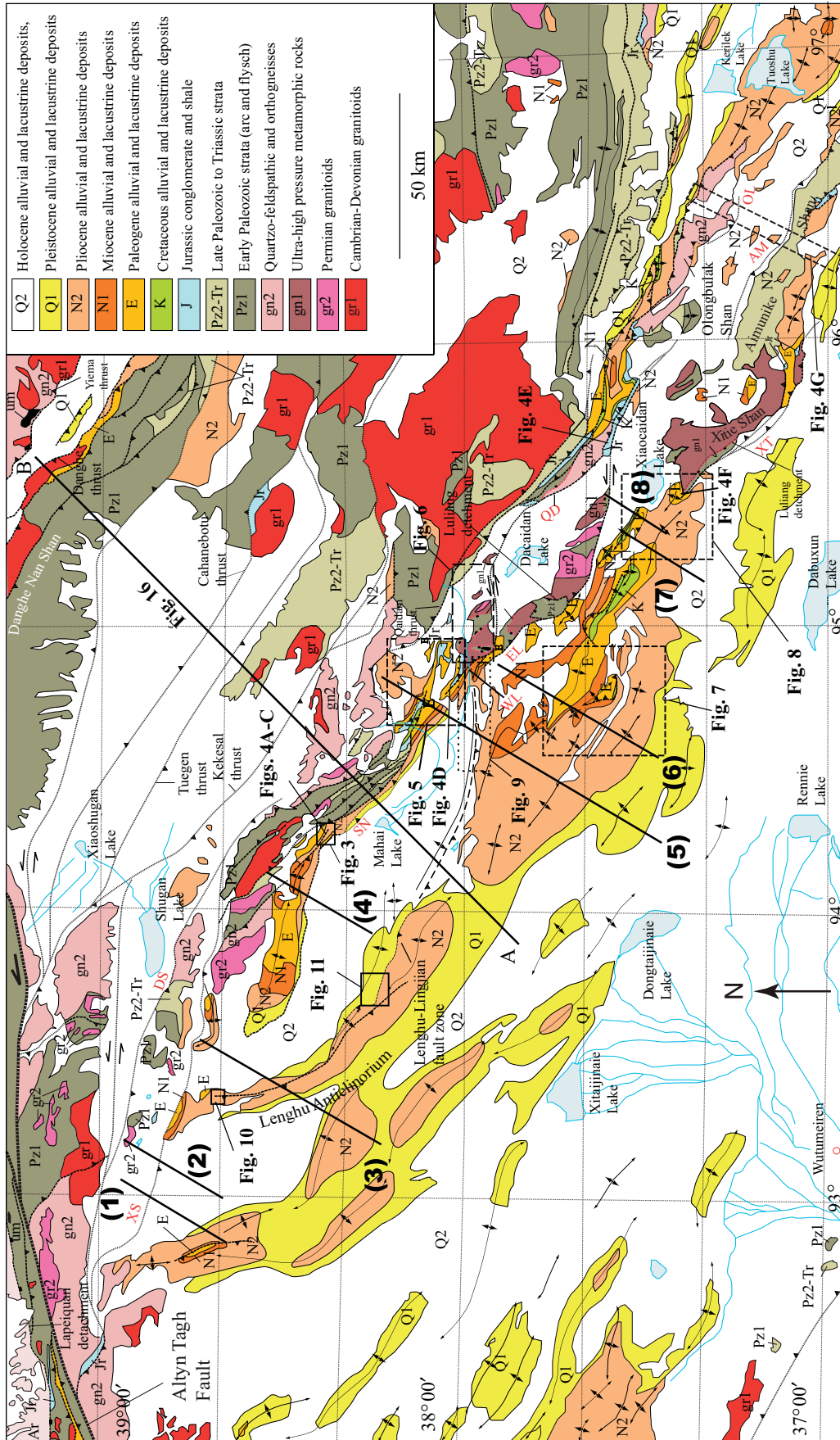


Figure 2. Geologic map of the southern Qilian Shan-Nan Shan thrust belt, modified from Liu (1988) based on our own observations. Line A–B is location of a regional geologic cross section shown in Figure 16. Locations of detailed geologic maps: Gaoquan area (Fig. 3), Lulehu area (Fig. 5), western Luliang Shan area (Fig. 6), Gaqiu area (Fig. 7), Xiaojimaie area (Fig. 8), Aimunik-Olongbulak section (A–O cross section) (Fig. 10), Lenghu-4 area (Fig. 10), Lenghu-6 area (Fig. 10), Lenghu-6 area (Fig. 10). Locations of field sketches in Figure 4 are also indicated. Numbers in parentheses denote locations of interpreted seismic reflection profiles (Fig. 13). Location of Fig. 12 coincides with line (1).

thrusts (Figs. 1B and 2). Along most of their traces the thrusts place Precambrian gneisses and early Paleozoic metagraywacke over Quaternary deposits (Fig. 2). The two faults merge to the east and west with their common western end linking with the left-slip Altyn Tagh fault (Fig. 1). The Dasaibe thrust is active, exhibiting prominent fault scarps and active foreland sedimentation in the footwall directly to the north (i.e., Sagan Lake; Fig. 2). As shown in seismic profiles (Figs. 13A and 13B) and our kinematic reconstructions (Fig. 15A), the thrust zone initiated in the Paleocene and early Eocene and acted as a passive roof thrust of a large south-

west-directed thrust duplex system; its development also produced an overlying southwest-thickening, growth-strata sequence (Figs. 13A and 13B).

Sainan Thrust Zone

The southwest-directed Sainan thrust zone is active and bounds an active foreland depocenter in its footwall to the south (Mahai Lake; Fig. 2). The thrust zone dies out to the east and west into folds involving Jurassic to Neogene strata. The western Sainan thrust zone in the Gaoquan area consists of six major northeast-dipping thrusts (Figs. 3A and 3B). The northernmost Gao-

quan thrust (fault-1) places Devonian strata (D) over Lower Jurassic strata (Jr1). Directly to the south, the Lower Jurassic strata are thrust over Middle Jurassic strata (Jr2) on fault-2, which in turn are thrust over the Paleocene to early Eocene Lulehe Formation (E1+2) on fault-3 (Fig. 3) (Table 1). The southern part of the section exposes three thrusts with down-dip striations (Fig. 4A): fault-4 places unit E3 over unit N1 with a complex structure in its hanging wall (Fig. 4B); fault-5 is an intra-formational thrust zone in unit E3 and its motion produced a fault-bend fold in the hanging wall (Fig. 4C); fault-6 (the Sainan thrust) juxtaposes middle Eocene to

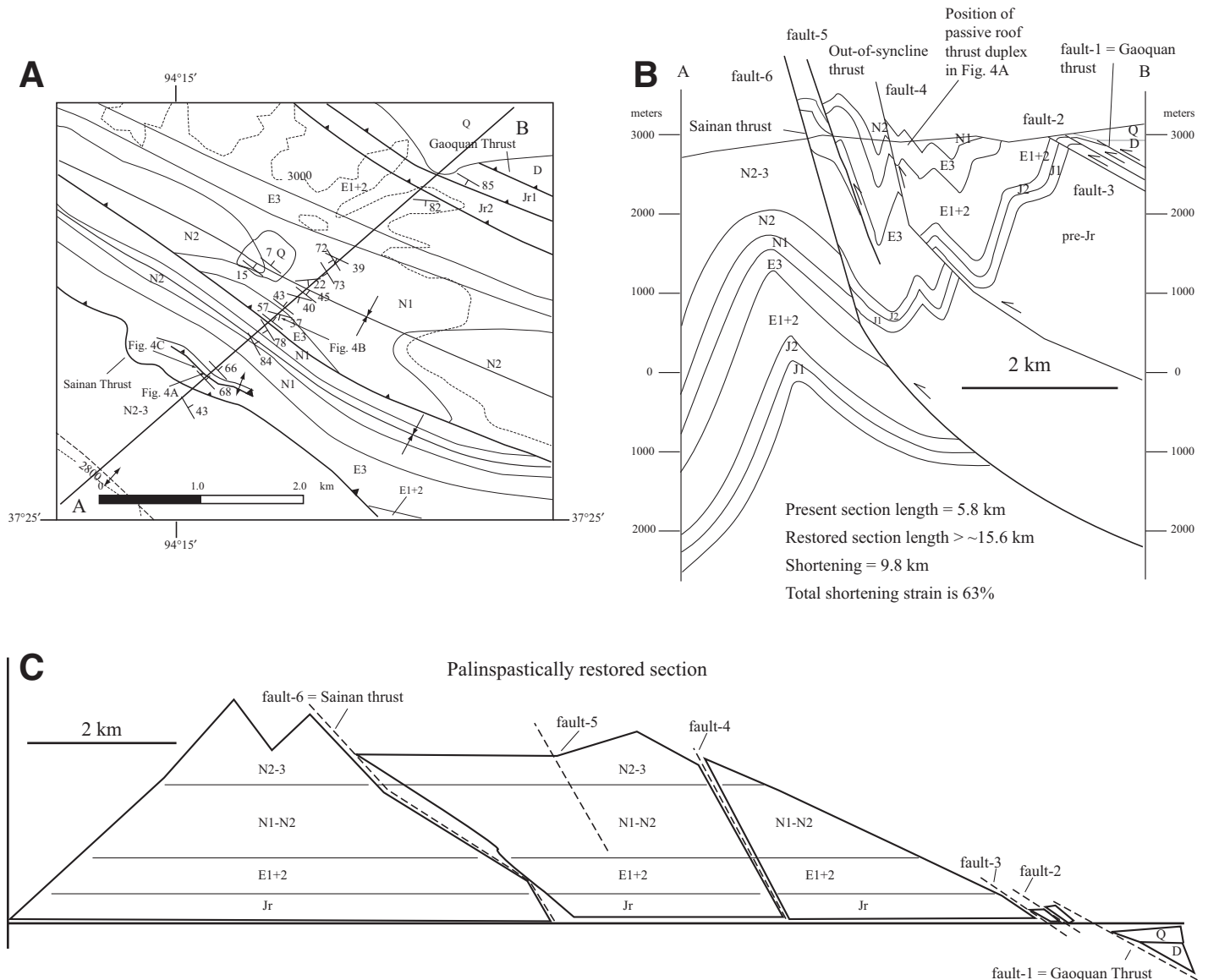


Figure 3. (A) Geologic map of the Gaoquan area; see Figure 2 for location. Locations of field photos in Figures 4A and 4B are also indicated. (B) Geologic cross section across Gaoquan area. See Figure 4A for location. See Table 1 for the definition of map units. Additional map symbols: Jr1—lower Jurassic, Jr2—middle Jurassic, D—Devonian. (C) Restored geologic cross section. (D) Kinematic reconstruction of the cross section shown in (A). (Continued on following page.)

Kinematic reconstruction

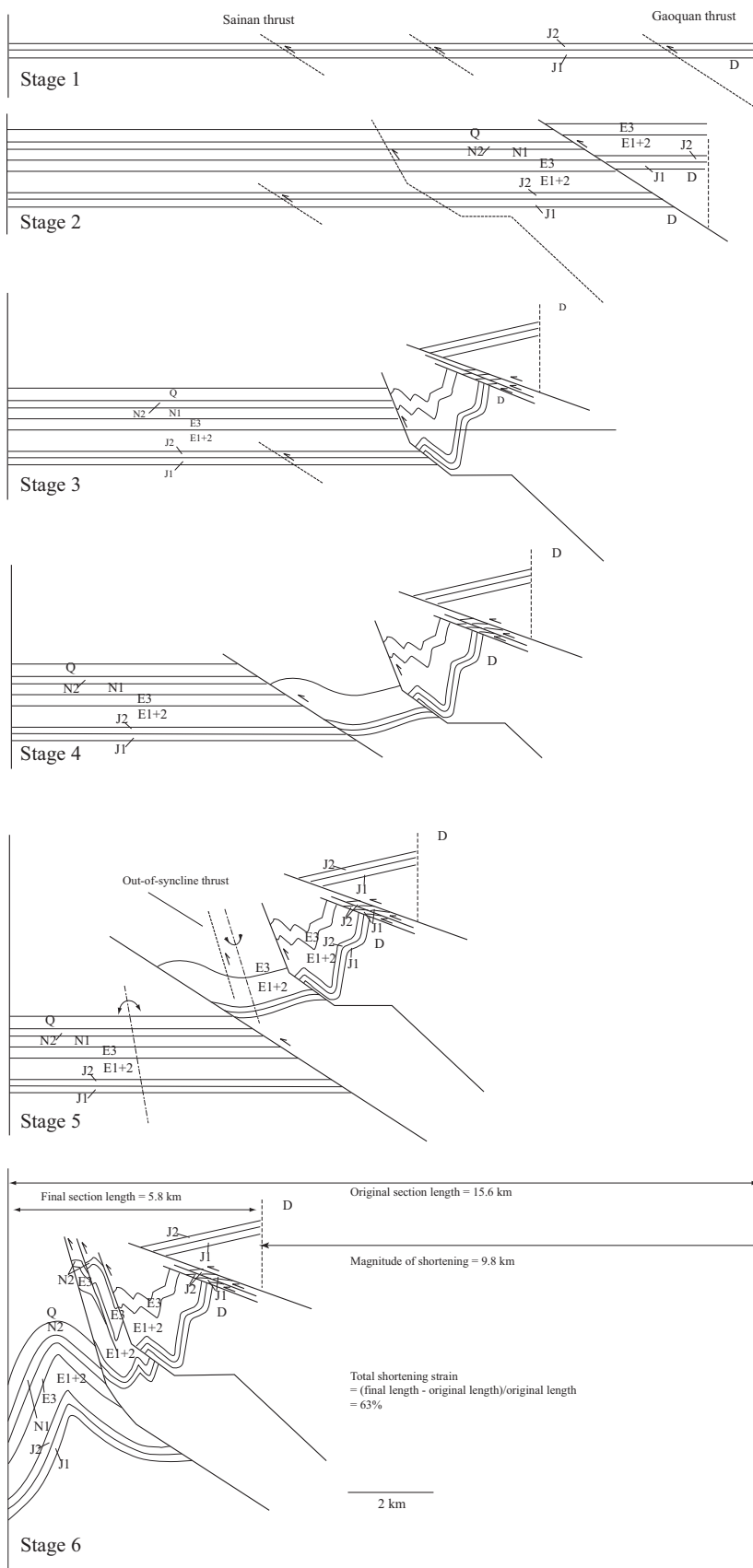


Figure 3 (continued).

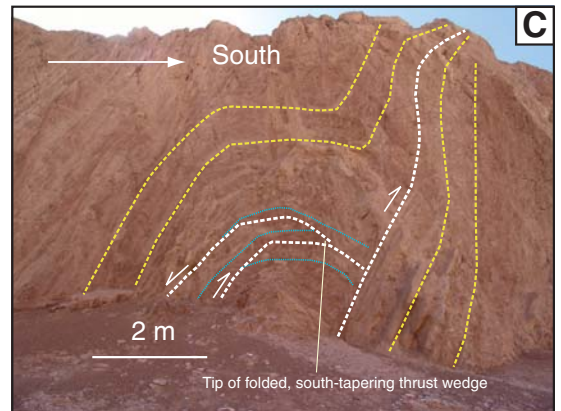
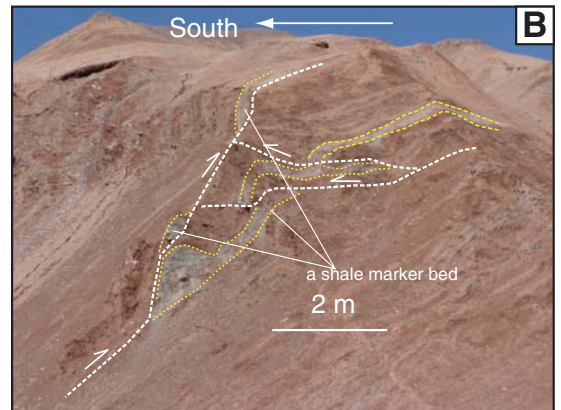
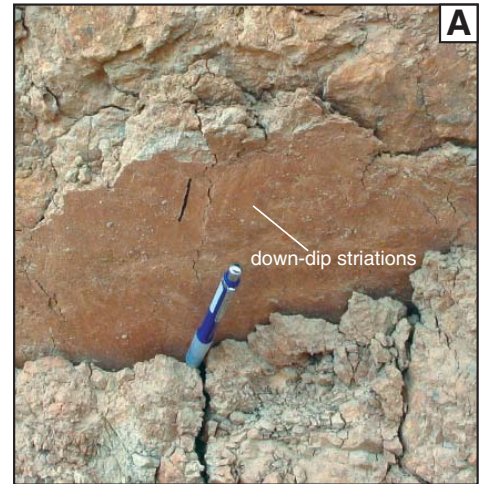


Figure 4. Field photos, sketches, and schematic cross sections; see Figure 2 for locations. (A) Down-dip striations on a thrust in Eocene red beds, Gaoquan area; see Figure 3A for location. (B) View northeast at southwest-directed minor thrusts truncated by a northeast-directed thrust in the middle Eocene to early Oligocene Xiagancaigou Formation (E3-1 + E3-2; see Table 1 for definition). Note complex distribution of a shale marker bed dismembered by two generation of thrusting with opposite sense of slip. (C) A fault-bend fold in the Xiagancaigou Formation (E3). See Figure 3A for location. (Continued on following page.)

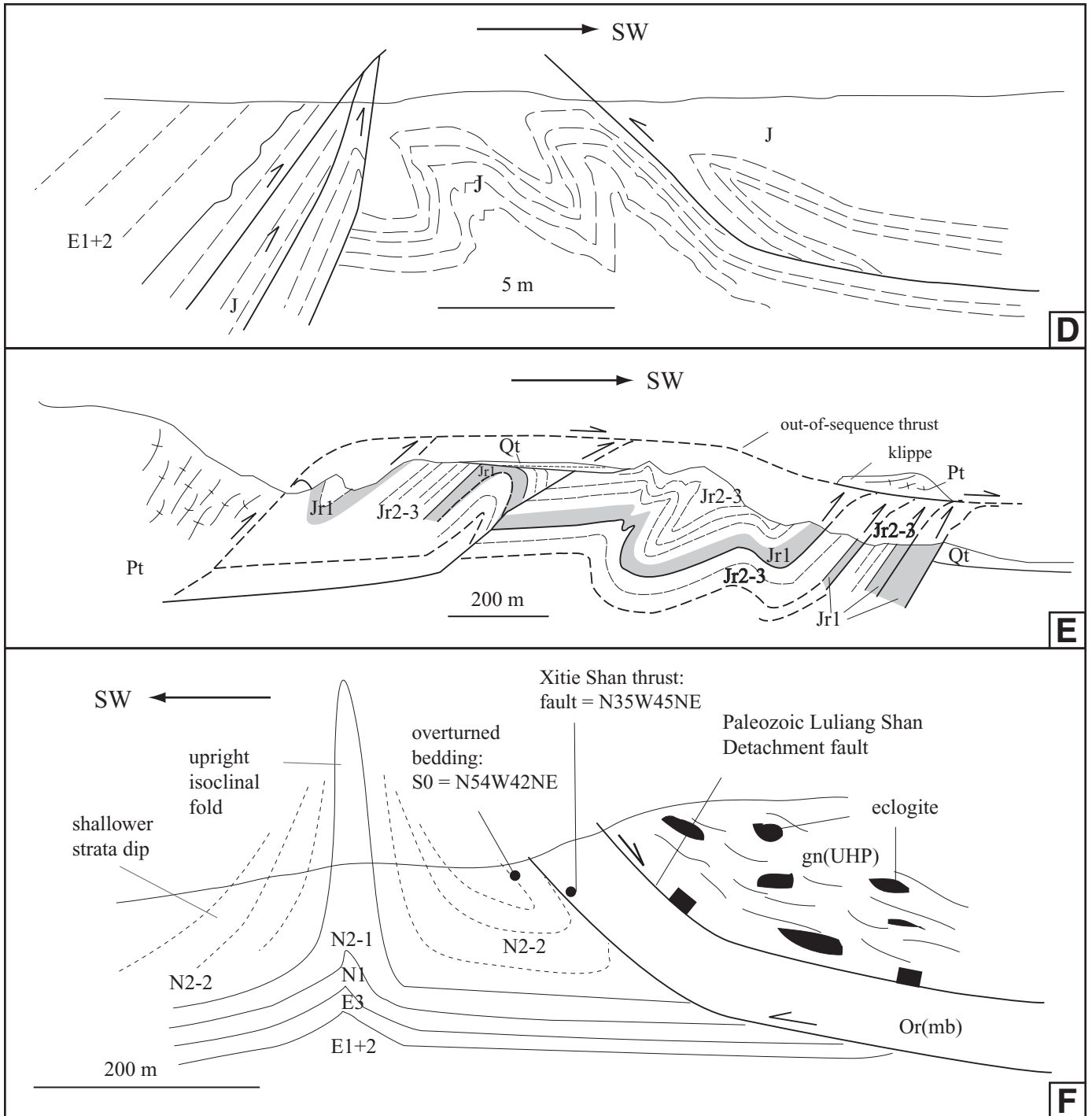


Figure 4 (continued). (D) Structure of the Qaidam Shan thrust zone along Lucaogou Valley, northern Qaidam Shan, constructed from a collage of photos. The structurally highest thrust carries Precambrian gneiss (Pt) above and truncates Jurassic strata below. Within Jurassic units, internal thrusts repeat Lower (Jr1) and Middle (Jr2) Jurassic formations. Note that the frontal thrust of the imbricate system remains active, causing uplift of a prominent Quaternary terrace (Qt) ~250 m above the active stream. (E) Complex thrusts and folds in the core of an anticline constructed from a field photo. This style of deformation is common in anticlines cored by Jurassic strata. (F) Field sketch of a detachment fold in the footwall of the Xitie Shan thrust. Note that Cenozoic strata are overturned directly below the thrust. The Luliang Shan detachment fault is a top-north, low-angle normal fault exhuming ultrahigh-pressure metamorphic rocks. At this locality, it is overturned and preserves top-north-shear indicators. The southern fold limb exhibits gentler dip, which could be induced either by hinge-zone thickening during folding or by the development of growth strata during a progressive increase in fold amplitude. (Continued on following page.)

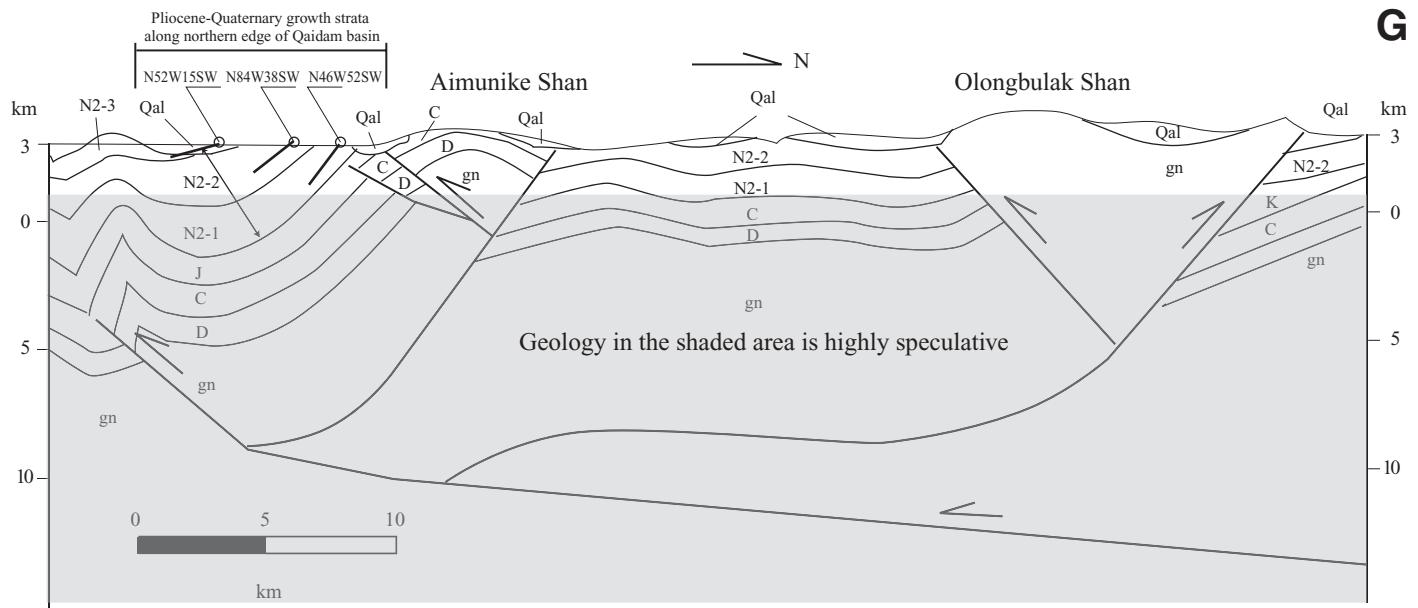


Figure 4 (continued). (G) Schematic cross section across the Aimunike Shan and Olongbulak Shan, shown as A–O cross section in Figure 2. Cenozoic map units are defined in Table 1. Additional units: gn—gneiss, D—Devonian, C—Carboniferous, J—Jurassic.

early Oligocene Upper and Lower Xiagancaigou Formations (E3) over Quaternary deposits (Q) (Figs. 3A and 3B). Palinspastic reconstruction of the cross section in Figure 3B indicates that the restored section was at least 15.6 km long, and had absorbed >63% of horizontal shortening (Figs. 3C and 3D). The minimum shortening estimate comes from the fact that the Devonian unit could lie in any position lower than that shown in Figure 3C, which would increase the estimated total shortening and the associated shortening strain.

The Sainan thrust zone extends eastward to the Lulehe area (Fig. 5), where it splits into two thrusts terminating into folds in the east. The termination folds overlap the trace of the Western Luliang thrust along strike to the south, which dies out westward into a Jurassic anticline. The core of the anticline is complexly deformed by top-north and top-south thrusts within Jurassic shale and sandstone directly below relatively little deformed unit E1+2 (Fig. 4D). North of the Sainan thrust zone is the Qaidam Shan thrust zone that juxtaposes Precambrian gneisses over Quaternary strata. Palinspastic restoration of the cross section in Figure 5B suggests that the section has absorbed at least 31 km of horizontal shortening, which yields a minimum shortening strain of 63% (Fig. 5C). Similar to the Gaoquan cross section in Figure 3B, there is no matching unit across the Qaidam Shan thrust, and the position of its hanging wall could be placed anywhere below that shown in the restored section in Figure 5C that would increase the shortening estimates. Our restoration requires the Qaidam

Shan thrust to have at least 23 km of fault slip in the area shown in Figure 8A.

Qaidam Shan Thrust Zone

This is the longest (~200 km) structure in the North Qaidam thrust system and has the most prominent topographic expression, with its hanging-wall elevation reaching ~5700 m and a structural relief locally exceeding 2 km across the fault (Figs. 1 and 2). The fault zone is active, as indicated by numerous fault scarps cutting Quaternary alluvial fans throughout its trace. The fault zone dies out in the hanging wall of the Xiaosaibe thrust in the west and in the footwall of the Olongbulak thrust in the east (Figs. 1 and 2). The Qaidam Shan thrust zone is also linked geometrically with three major thrust zones to the south: the Sainan, Western Luliang, and Eastern Luliang thrusts (Figs. 1B and 2). The Qaidam Shan thrust zone consists of imbricate thrusts placing Precambrian gneiss over Jurassic strata and Jurassic strata over Quaternary deposits (Fig. 4E). Active thrusting along the Qaidam Shan thrust zone has raised Quaternary strath terraces in the hanging wall ~150 m above the active streams (Fig. 4E).

Luliang Shan Thrust Zone

The Luliang Shan thrust zone consists of the Western and Eastern Luliang thrusts, both exhibiting L-shaped geometry in map view with the northwest-striking thrust segments linking with the east-northeast-striking lateral ramp segments (Figs. 1B and 2). The lateral ramps

are active, as expressed by fault scarps along the fault traces and the development of the active depocenters directly against the faults (i.e., the Daqaidam Lake against the western Luliang lateral ramp and Xiaoqaidam Lake against the Eastern Luliang lateral ramp). Folds in the Mesozoic and Cenozoic strata and synforms in the Luliang Shan high-grade gneisses share the same axes (Fig. 6), a relationship suggesting that the crystalline basement did not behave as rigid blocks. Palinspastic reconstruction of a cross section through the area indicates >34-km horizontal shortening and a shortening strain of >55%. Minimum slip on the Qaidam Shan thrust is 11 km (Fig. 6C).

Structures south of the Luliang Shan thrust zone are mapped in the Gaqiu area (Fig. 7A), where several south-directed thrusts are cut by younger north-trending, left-slip faults and northeast-trending, right-slip faults (Fig. 7A). Although both thrusts and strike-slip faults accommodate northeast-southwest shortening, they reflect a temporal change in the state of stress. The intermediate principal stress axis was horizontal during early thrusting and changed later to a vertical orientation during strike-slip faulting. Palinspastic reconstruction of a cross section through the area requires >22-km horizontal shortening and a shortening strain of >38% (Fig. 7C).

Xitie Shan Thrust Zone

The Xitie Shan thrust is a northeast-dipping, basement-involved structure that dies out into folds laterally toward the Luliang Shan to the

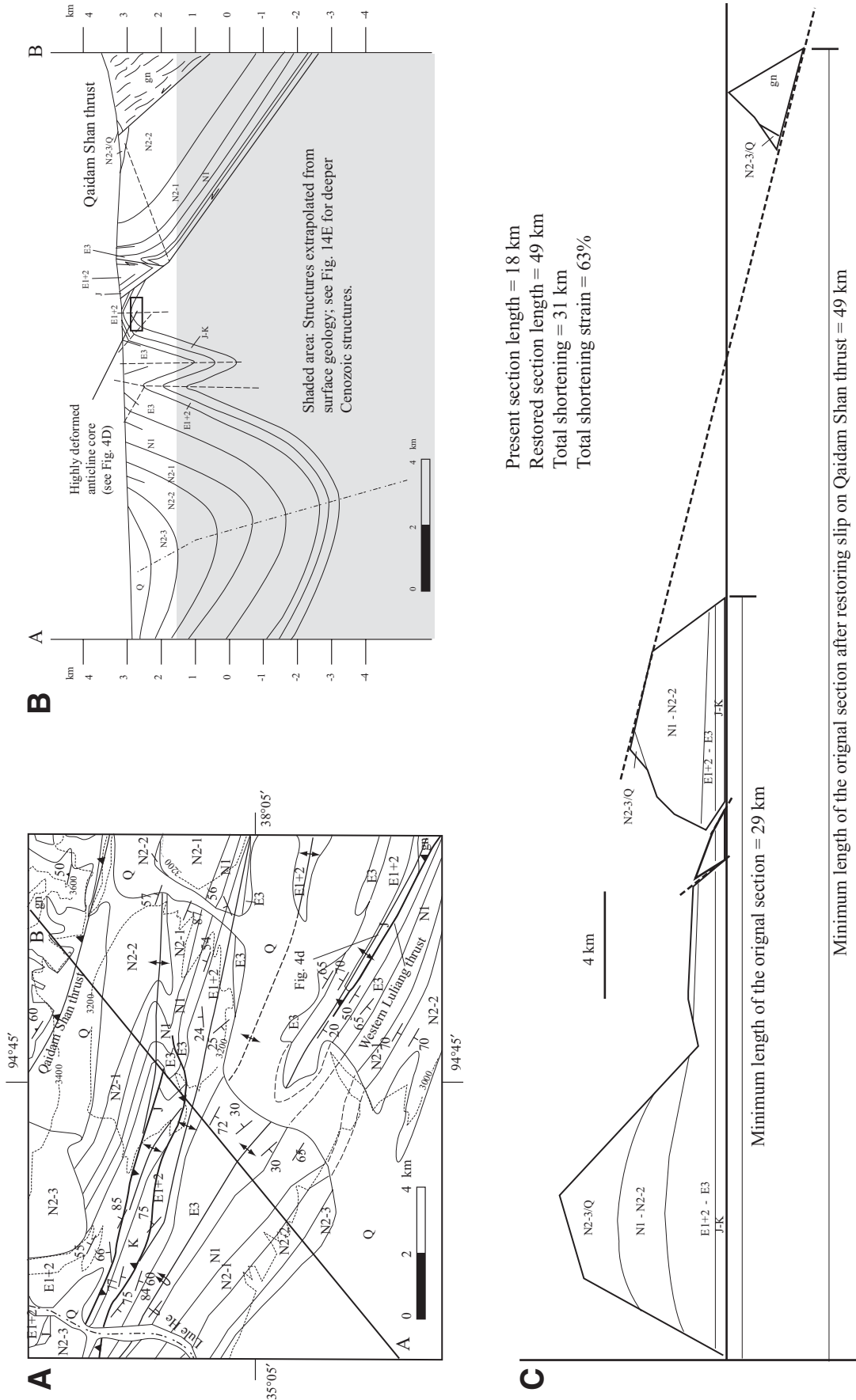


Figure 5. (A) Detailed geologic map of the Lulehe area. (B) Geologic cross section: gn—gneisses; see Table 1 for definition of other map units. (C) Restored section.

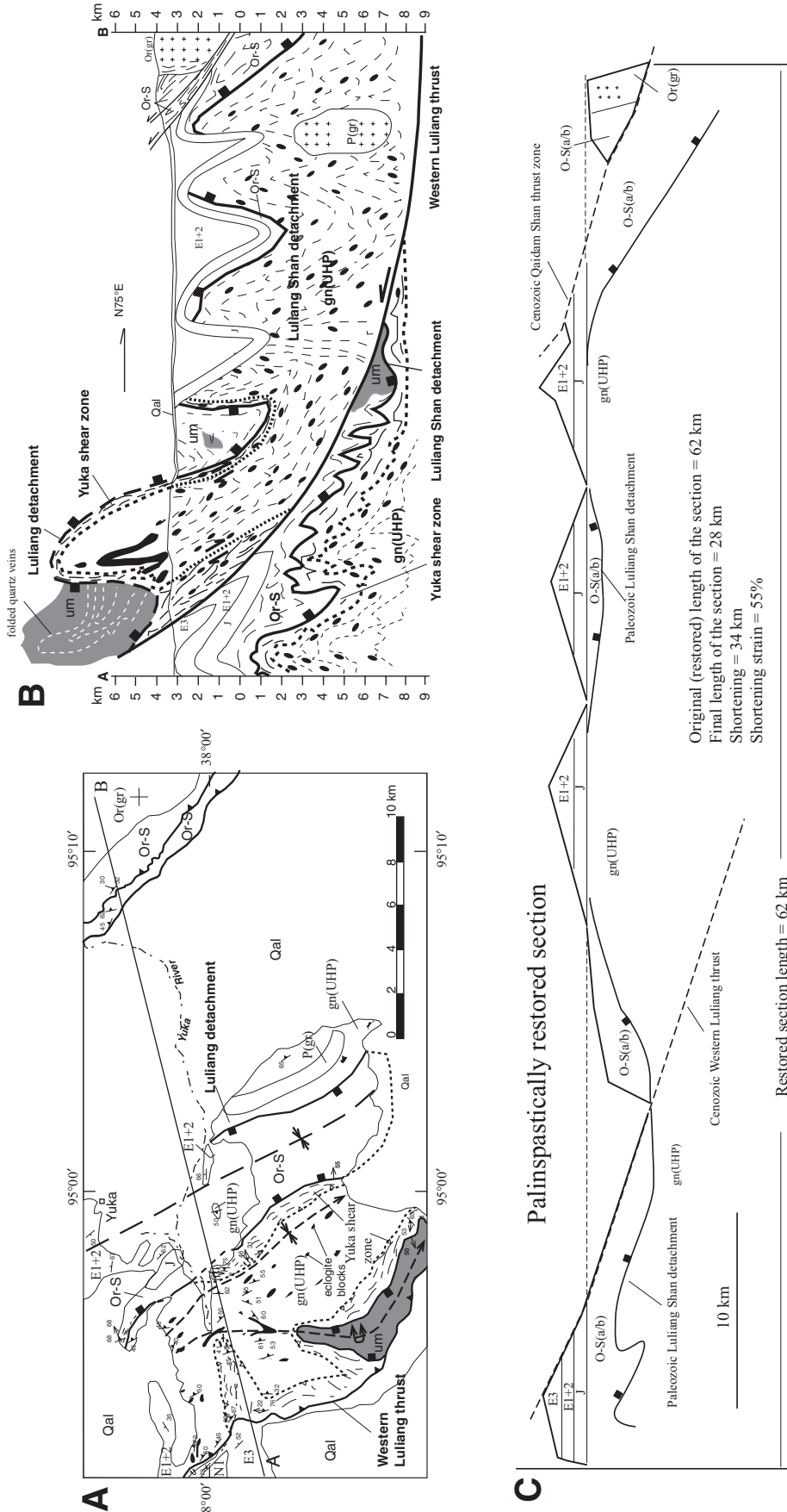


Figure 6. (A) Detailed geologic map of the western Luliang Shan area; see Figure 2 for location and Table 1 for definition of map units. Additional units: Or-S—Ordovician metasedimentary and metabasite, gn(UHP)—ultrahigh-pressure metamorphic rocks; um—ultramafic rocks, P(gr)—Permian granite, Or(gr)—Ordovician granite. (B) Geologic cross section. (C) Restored section.

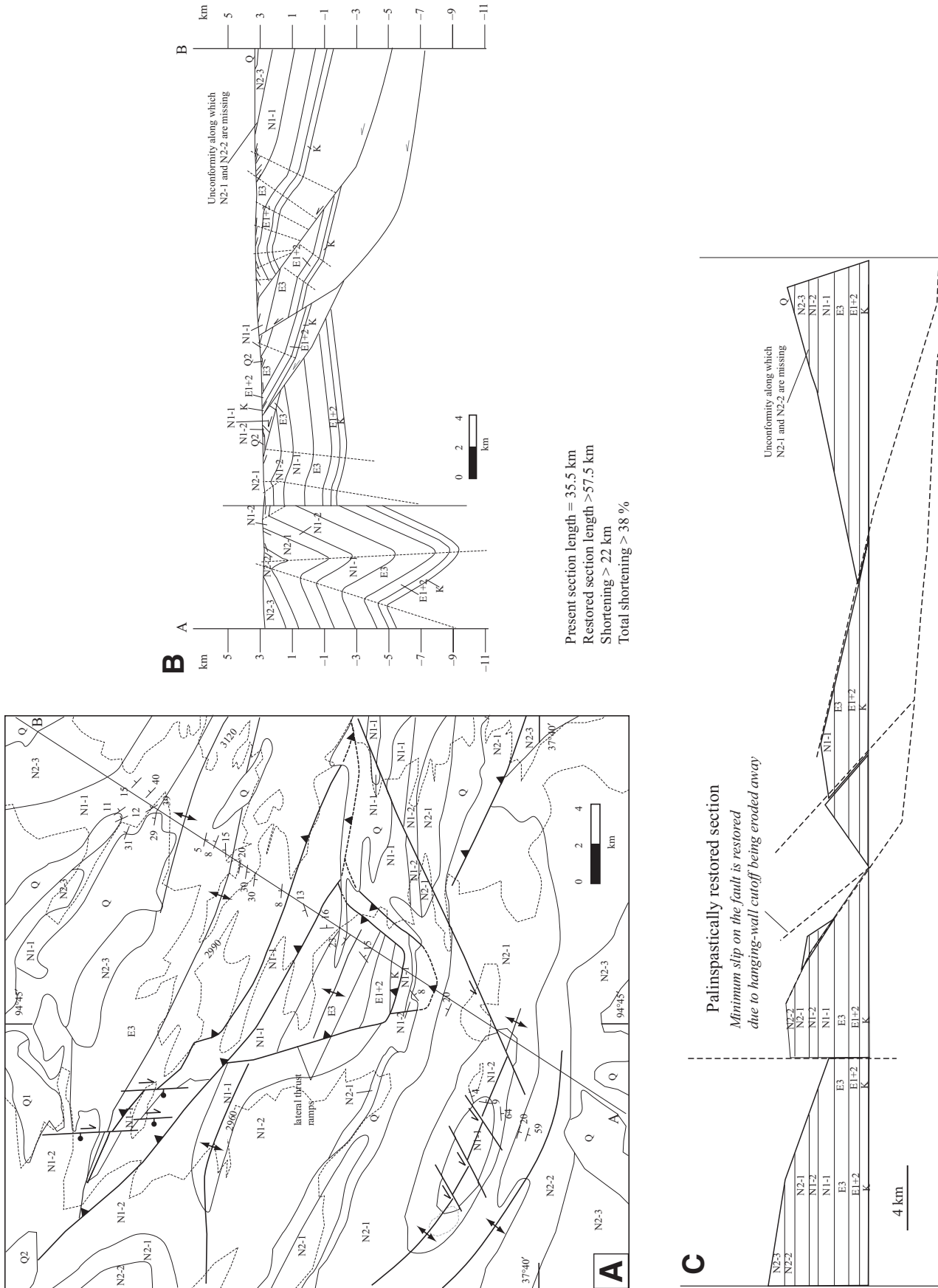


Figure 7. (A) Detailed geologic map of the Gaqiu area; see Figure 2 for location. (B) Geologic cross section. Total shortening exceeds 38%. See Table 1 for definition of Cenozoic unit. K—Cretaceous.

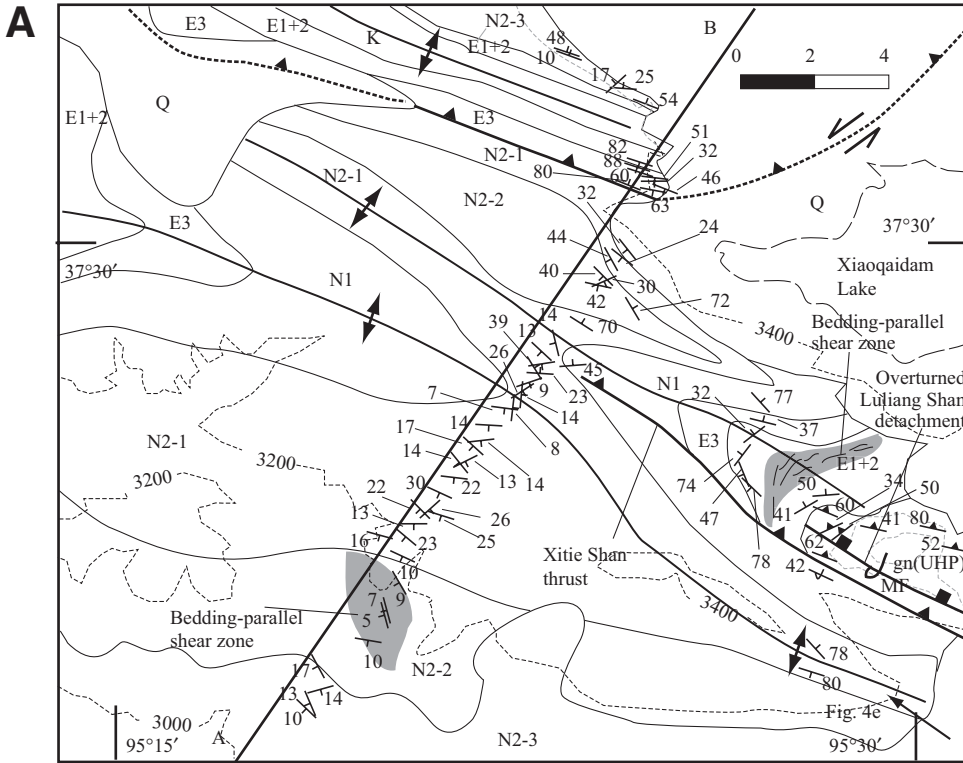
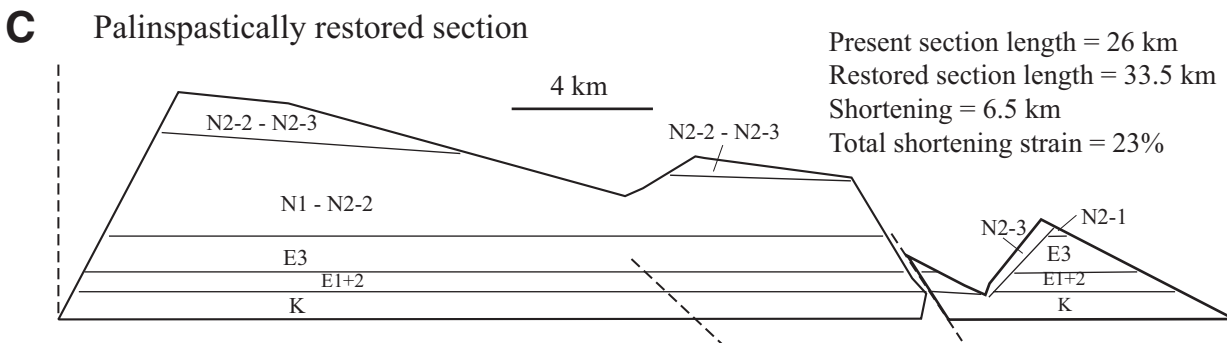
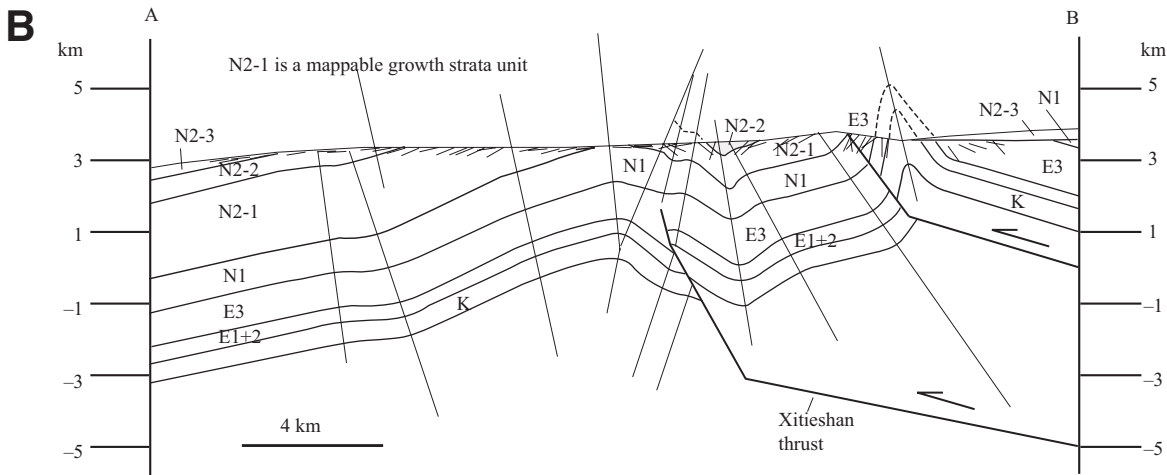


Figure 8. (A) Detailed geologic map of the Xiaoqaidam area. Bedding parallel shear zones are observed in units E1+2 and N2-2. gn(UHP)—ultrahigh-pressure metamorphic rocks. (B) Geologic cross section. N2-1 unit displays southward thickening, which is interpreted as growth strata associated with anticlinal folding above the Xitie Shan thrust (i.e., Xitie Shan thrust was active during deposition of unit N2-1). (C) Restored section.



west and Aimunik Shan to the east (Fig. 2). Along the northern limb of the western termination anticline, bedding-parallel shears are widely developed in units E1+2 and N2-2, across which bed dips vary significantly (Fig. 8A). Along the southern limb, growth strata are well developed as indicated by progressive southwestward thickening of unit N2-1 (Fig. 8B). This relationship requires the Xitie Shan thrust to be active during the early to middle Miocene and is broadly consistent with the seismic data that contractional deformation in the same area was initiated during early Oligocene deposition (Fig. 13H). A tight, upright anticline is developed in the footwall of the Xitie Shan thrust. It has nearly vertical limbs at the fold core and progressively shallower limbs away from the fold hinge zone (Fig. 4F). The lack of intraformational deformation and the presence of progressive thickening of individual beds observed in the field led us to conclude that the shallowing of the fold limbs was produced by synchronous folding (Fig. 4F). Palinspastic reconstruction of the cross section in Figure 8B requires 6.5-km horizontal shortening and a shortening strain of ~23% (Fig. 8C).

Aimunik and Olongbulak Thrusts

Although Paleogene strata are preserved in the Xitie Shan area, they are missing in the Aimunik Shan directly to the east (Figs. 2, 4G, and 8). There, only Neogene strata unconformably over Devonian-Carboniferous and Jurassic strata are present. The eastward overlapping of Neogene strata over pre-Cenozoic rocks from the Xitie Shan to the Aimunik Shan is consistent with the observation that Qaidam basin has been expanding eastward during the Neogene (Huang et al., 1996; Wang et al., 2006). A narrow, northwest-trending Neogene basin is located between the north-dipping Olongbulak thrust in the north and the south-dipping Aimunik thrust in the south. This basin could be part of a much larger Qaidam basin and was later incorporated into the southern Qilian Shan-Nan Shan thrust belt during the development of the Aimunik thrust. The Aimunik thrust dies out to the west into a fold complex in the Xitie Shan and to the east into the Changshan anticline (Figs. 1B and 2). The Olongbulak thrust dies out to the west into a fold complex linked with the Qaidam Shan thrust zone and terminates to the east at the Dalang anticline (Figs. 1 and 2).

Lenghu Anticlinorium

The anticlinorium is truncated by the Xiaosai-bei thrust in the west and terminates at the Western Luliang thrust in the east. The fold is arcuate in map view, with a rectilinear northwest segment and a curvilinear southeast segment. The Lenghu-Lingjian thrust zone (Figs. 9, 10, and 11) is part of a passive roof thrust zone above a southwest-directed thrust wedge. The relationship between the Lenghu anticlinorium and the Western Luliang thrust is similar to that between the Luliang Shan thrust zone and the Qaidam Shan thrust zone, both having the lateral ramps to merge with an overriding thrust (Fig. 2). A key difference between them is that the Lenghu-Lingjian lateral ramp is blind below an anticline while the Luliang lateral ramps are all exposed at the surface. Deformation associated with the fold above the Lenghu-Lingjian thrust has caused the Western Luliang thrust to be overturned with a local southward dip (Fig. 9).

We mapped surface structures of the Lenghu anticlinorium in two places (Fig. 2). In the Lenghu-4 area (Fig. 10), the south-dipping Lenghu-Lingjian thrust zone places Miocene strata over Pliocene strata. Palinspastically restored section

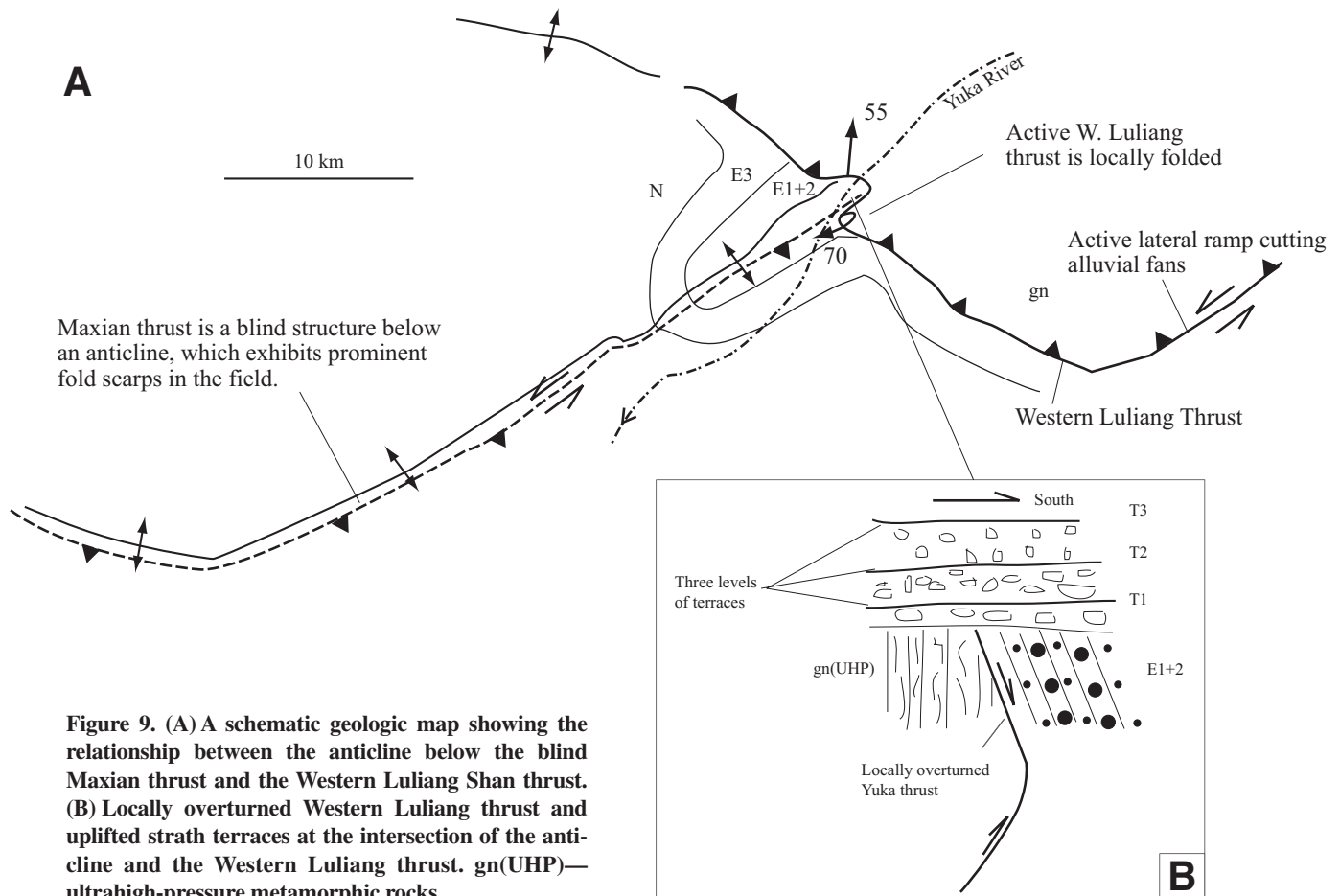


Figure 9. (A) A schematic geologic map showing the relationship between the anticline below the blind Maxian thrust and the Western Luliang Shan thrust. **(B)** Locally overturned Western Luliang thrust and uplifted strath terraces at the intersection of the anticline and the Western Luliang thrust. gn(UHP)—ultrahigh-pressure metamorphic rocks.

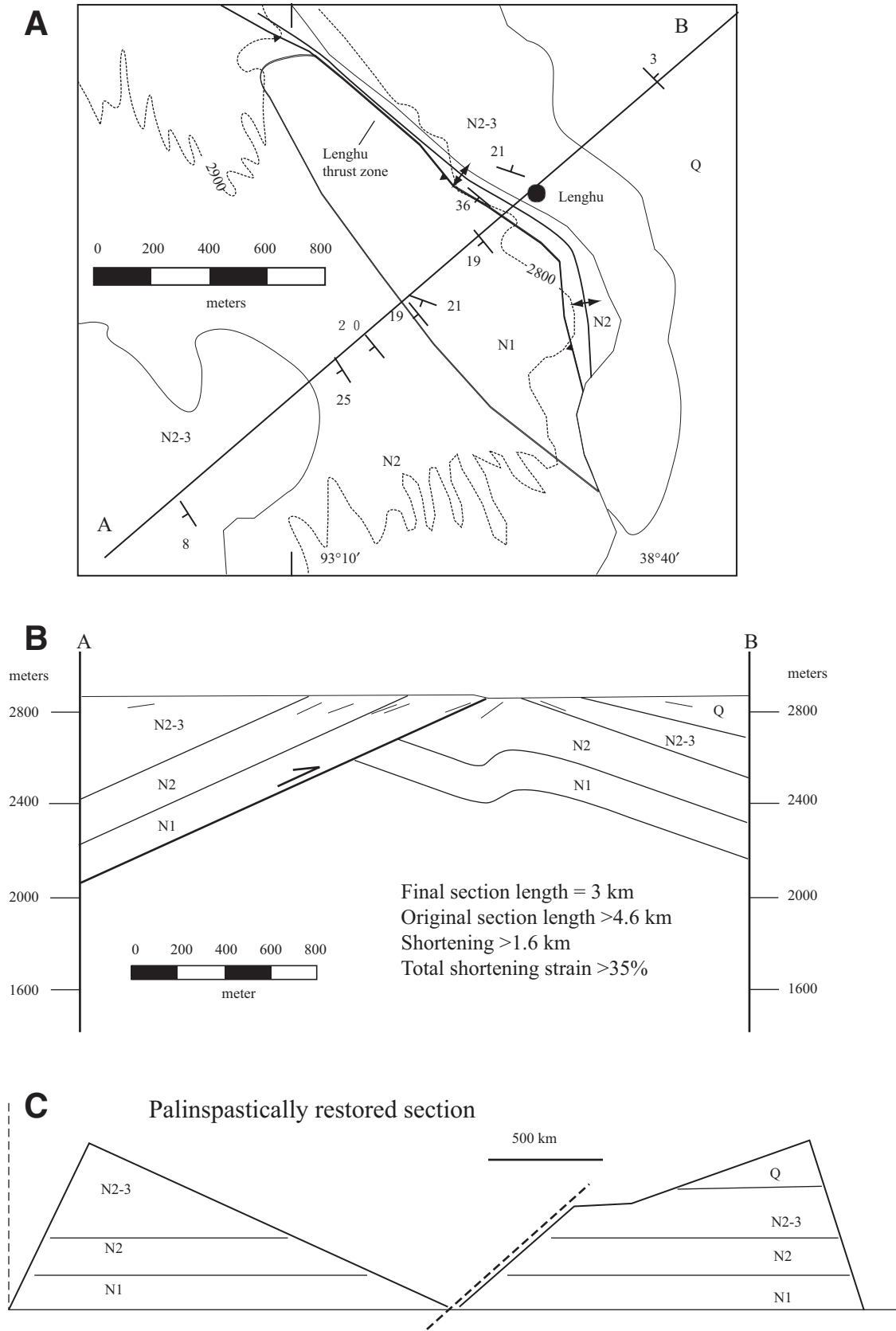


Figure 10. (A) Detailed geologic map of the Lenghu-4 area. (B) Geologic cross section. See Table 1 for definition of Cenozoic units. (C) Restored section.

requires >1.6-km horizontal shortening and a minimum strain of ~35% (Fig. 10C). In the Lenghu-6 area (Fig. 11), the south-dipping Lenghu-Lingjian thrust zone is developed in the Neogene strata, with a tight, southwest-verging anticline in its footwall of the northeast-directed thrust. This relationship leads us to interpret that thrusting postdates the footwall fold. Bedding-parallel shear zones are common in Neogene units. Palinspastic restoration of a cross section across the area requires 16-km horizontal shortening and a shortening strain of ~39% (Fig. 11C).

Subsurface Geology of Northern Qaidam Basin

Although the laterally overlapping relationships among thrusts and their termination folds in the North Qaidam thrust system suggest their coeval development and kinematic linkage, the geometric relationships in map view alone do not permit the establishment of the timing and sequence of deformation across the thrust system. In addition, surface mapping does not provide a complete picture of the upper crustal structures in northern Qaidam basin. To resolve these problems we have acquired and interpreted more than 100 individual seismic reflection profiles across northern Qaidam basin. Our seismic interpretations were also assisted and verified by drill-hole data. Below we select eight sections to illustrate the style, magnitude, and timing of Cenozoic deformation (Fig. 2). In order to construct true-scale geologic cross sections, we first interpret seismic profiles in the time domains, which were then converted to depth sections by assigning known depth-dependent velocity distributions. An example of interpreted time sections is shown in Figure 12. All interpreted seismic profiles use a reference elevation of 2750 m (the lowest point of Qaidam basin) as the zero-km depth.

Seismic Profile (1) (Fig. 13A)

This section exhibits a growth-strata relationship for the whole Cenozoic sequence, which thickens to the southwest toward the basin axis. The section also displays nested southwest-tapering, thrust-duplex wedges (triangle zones, *a la* Price, 1986). At the surface, the northeast-directed roof thrust zone correlates with the southwest-dipping Xiaosaibe thrust, whereas the south-directed imbricate zone below correlates with the northeast-dipping Sainan thrust zone. The oldest unit in the growth strata is the Paleocene to early Eocene Lulehe Formation (E1+2), suggesting the initiation of the triangle zone occurred at this time. The northward-tapering, growth-strata sequence (GS-1, Fig. 13A) is subsequently folded by a syncline, which was

in turn associated with a younger sequence of growth strata with an age range from the late Miocene to Pliocene (units N2-2 and N2-3 in GS-2, Fig. 13A). Palinspastic reconstruction of the section requires 26-km horizontal shortening with a shortening strain of ~34% (Fig. 13A).

Seismic Profile (2) (Fig. 13B)

This section has a similar structural style to that in section (1), exhibiting a large triangle zone and an overlying growth-strata sequence. Again, as in Figure 13A, the northeast-directed passive-roof fault correlates with the Xiaosaibe thrust and the southwest-directed imbricate zone below correlates with the Sainan thrust zone. The northeast-tapering, growth-strata sequence is folded by two later synclines, each generating its own growth strata in the fold cores. The northern late syncline started to develop during deposition of unit E3-1 (GS-1, Fig. 13B), while the southern late syncline started to develop during deposition of unit N1 (GS-2, Fig. 13B). These temporal relationships again indicate southward propagation of shortening deformation across northern Qaidam basin. This interpreted deformation pattern is consistent with the observation that backthrusts from the southern part of the section cut and offset the thrusts in the northern part of the section (Fig. 13B). Palinspastic reconstruction of the section requires 19-km horizontal shortening and a shortening strain of ~36%.

Seismic Profile (3) (Fig. 13C)

This section shows a thrust-wedge duplex (triangle-zone structure) in the north and two widely spaced, southwest-directed thrusts in the south. The floor thrust of the duplex is part of the Sainan thrust zone that is also imaged seismically in profiles (1) and (2) (Figs. 13A and 13B). The roof thrust is passive, linking with the northeast-directed Xiaosaibe thrust zone. As in sections (1) and (2), the entire Cenozoic sequence thickens southwestward directly above the thrust duplex, indicating its development started during the deposition of unit E1+2 and lasted until at least the late Oligocene during deposition of unit N-1. The southern thrusts were developed after the initiation of the triangle zone to the north, as their related folds deformed the southwest-thickening growth-strata sequence between unit E1+2 and N2-1. The younger southwest-directed fault-1 started to develop during deposition of unit N2-2 in the late to middle Miocene (Fig. 13C), again suggesting the deformation front migrated southward toward the basin interior. A small, south-dipping normal fault is present in the Jurassic strata, producing a small half graben. Palinspastic reconstruction of the section requires 26 km of shortening and a shortening strain of 29%.

Seismic Profile (4) (Fig. 13D)

This section crosses the Sainan thrust zone and consists of geometrically linked bivergent thrust wedges stacking on top of one another. The northeast-directed thrusts in the profile are parts of the passive-roof fault zone as imaged in profiles (1) to (3) (Figs. 13A–13C), but with a significantly decreased magnitude of slip, only on the order of hundreds of meters versus greater than a few kilometers of slip as in the other sections. Southwestward thickening of Cenozoic strata remains evident in the section and can be divided into two growth-strata sequences. The northern sequence (GS-1) includes units E1+2 to N2-2, whereas the southern sequence contains units E3-2 to N2-2, with unit E3-2 (early Oligocene) having the most prominent variation in thickness. We interpret deposition of the GS-1 during motion on fault-2 and deposition of the GS-2 during motion on fault-1 in the Sainan thrust zone. The growth-strata relationships again suggest that the deformation front has migrated southwestward across northern Qaidam basin. Palinspastic reconstruction of the section requires 10-km horizontal shortening and a shortening strain of ~21%.

Seismic Profile (5) (Fig. 13E)

This section crosses the north-dipping Sainan thrust zone and the lateral ramp segment of the south-dipping Lenghu-Lingjian fault zone. The two faults bound a blind pop-up structure below the Lenghu anticlinorium. The hanging wall of the Lenghu-Lingjian thrust also forms a northeast-tapering thrust wedge that is bounded by a top-southwest thrust lying mostly within unit N2-1. The Paleogene sequence in this section is thinner than that in sections (1) to (4). A synclinal trough is developed between the Sainan and Lenghu-Lingjian thrusts, with unit E3-1 as a prominent growth-strata sequence in their common footwall. This relationship indicates that motion on the Lenghu-Lingjian and Sainan thrusts started in the middle to late Eocene during deposition of unit E3-1. This age is slightly younger than the onset age of Cenozoic deformation in sections (1) to (4) in the Paleocene to early Eocene during deposition of unit E1+2. The synclinal folding is active as indicated by the presence of Holocene growth strata in its core. The section also shows that units E3-2 (early Oligocene) to N1 (late Oligocene) have constant thickness, whereas units N2-1 (early to middle Miocene) to Q (Quaternary) exhibit growth-strata geometry across the anticlinorium on its limbs. The latter relationship suggests that motion on the Lenghu-Lingjian fault zone ceased in the early Eocene but was later reactivated in the early Miocene, with a dormant period of ~25 m.y.!

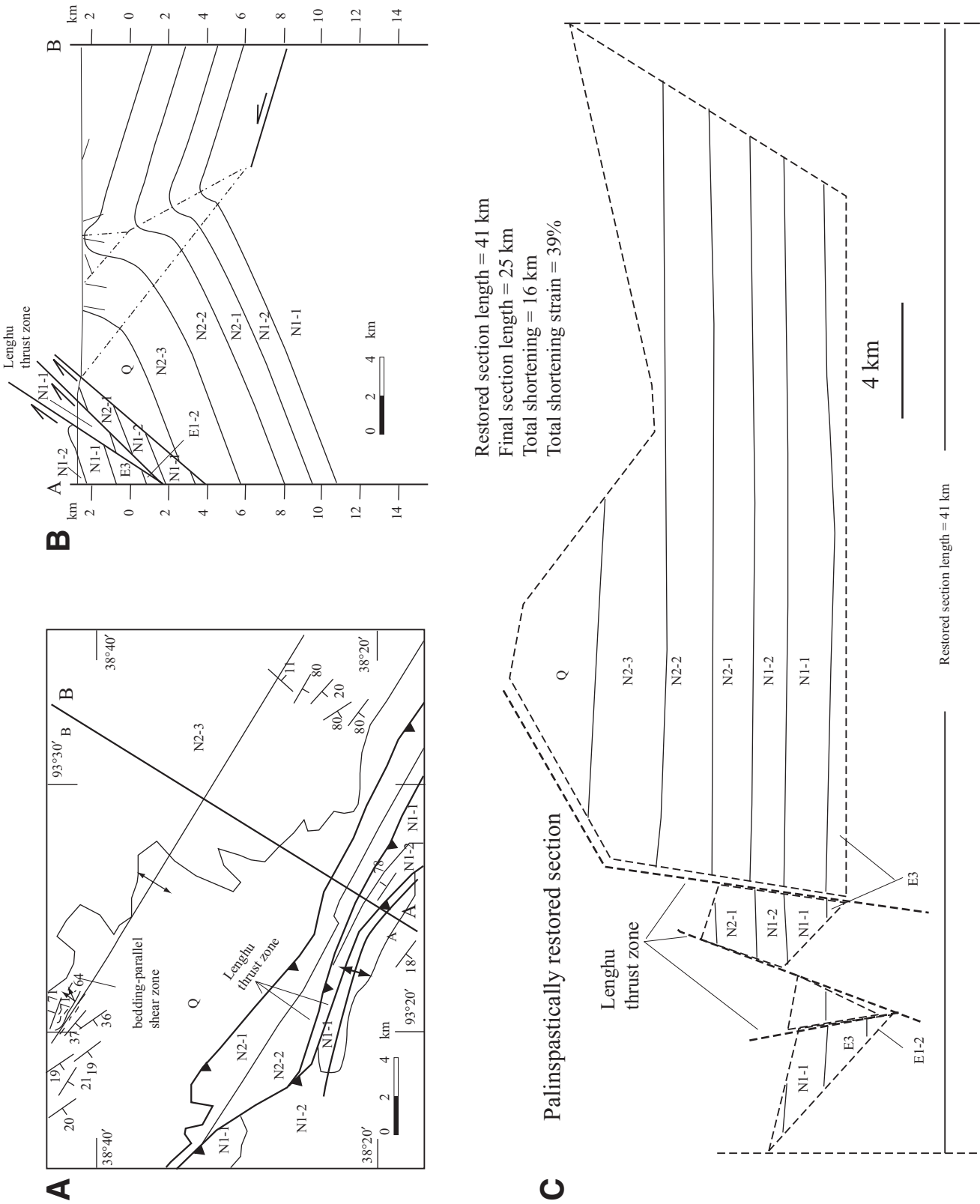


Figure 11. (A) Detailed geologic map of the Lenghu-6 area. (B) Geologic cross section. See Table for definition of Cenozoic units. (C) Restored section.

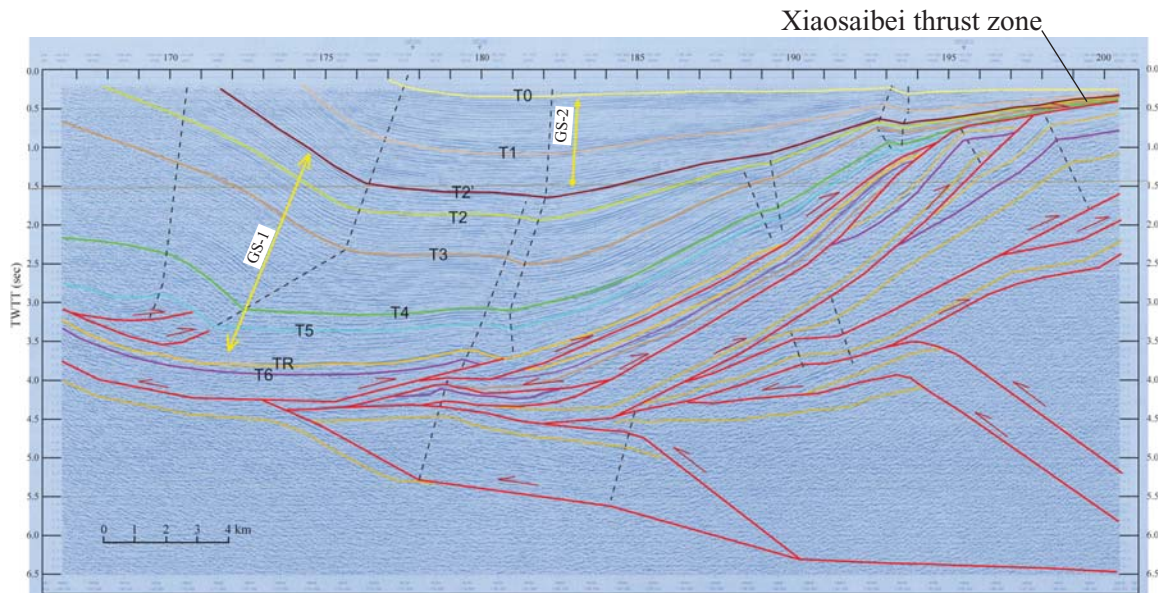


Figure 12. Interpreted seismic profile (1) in time domain. T0 to T6 are regionally correlative reflectors; T0 at the top of the Shizigou Formation, T1 at the top of the Shangyoushan Formation, T2 at the top of the Xiayoushan Formation, T3 at the top of the Shangganchaigou Formation, TR at the top of the Lulehe Formation, and T6 at the top of the Jurassic-Cretaceous strata. GS-1 and GS-2 are two growth-strata sequences associated with the development of the triangle zone and later synclinal folding. TWTT—two-way travel time.

Several north-dipping, normal-separation faults are present in the Jurassic strata or bounding basins containing Jurassic strata, with slip varying from a few hundreds of meters to ~2 km. Half grabens are developed in the hanging walls of the normal-separation faults. A major gliding horizon is present in the Jurassic strata, along which a thrust duplex is developed. Palinspastic reconstruction of the section requires 46-km horizontal shortening and a shortening strain of ~31%. Because section (5) passes through our mapped area shown in Figure 5, we compare the overlapping segments of the field-based cross section (Fig. 5B) and seismically based cross section (Fig. 13E), respectively. It is clear that the field-based cross section can only capture the structural geometry in the uppermost few kilometers of the section. It is also clear that the steep bed dips do not penetrate deep in the crustal section, because fold limbs in the deeper part of the seismic section have much shallower dips than those measured at the surface.

Seismic Profile (6) (Fig. 13F)

This section crosses a southwest-directed, imbricate thrust zone, with fault-1 at the highest structural level. In the fault-1 hanging wall unit, E1+2 is significantly thicker in the core of a syncline that is unconformably overlain by unit E3-1. The syncline and unit E3-1 are both cut by fault-1. Across fault 1, unit E1+2 is thinner in its footwall than that in its hanging wall,

while unit E3-1 is thicker in the footwall and that in the hanging wall. The above relationships suggest that fault-1 was initiated after deposition of unit E1+2 and during deposition of unit E3-1. In the footwall of fault-1, units E1+2 and E3-1 exhibit prominent thinning in the hanging walls of fault-2 and fault-3, suggesting that the faults were active during their deposition in the Paleocene and Eocene. The above relationships suggest two sequential deformation events. First, a broad syncline was developed during deposition of unit E1+2 associated with motion on fault-2 and fault-3 below. Fault-1 was developed later during deposition of unit E3-1 as an out-of-sequence thrust. Continuous motion on fault-1 had created a northeast-tapering growth-strata sequence during deposition of unit N2-2 in the southernmost part of the section (Fig. 13F). Palinspastic reconstruction of the section requires 29-km shortening and a shortening strain of ~27%.

Seismic Profiles (7) and (8) (Figs. 13G and 13H)

Sections (7) and (8) record a southwestward younging deformation history along a north-south transect. Section (7) represents the southern transect, while section (8) represents the northern transect. Major structures in section (7) include a northeast-directed, fault-bend fold system and a south-directed, roof fault zone on top of the fault-bend fold to the north. Two

detachment horizons are developed in the Jurassic and early Oligocene units (Jr and E3-2), along which fault-bend folds and imbricate thrusts are branched off. Only unit Q exhibits a growth-strata relationship, suggesting structural development in the Quaternary. Palinspastic reconstruction of section (7) (Fig. 13G) requires 50-km horizontal shortening and a shortening strain of ~58%.

In contrast to section (7), the initiation age of deformation in section (8) is significantly older, and occurred in the early Oligocene as illustrated by thickness variation of unit E3-2 overlying a thrust wedge (Fig. 13H). Due to the presence of bedding-parallel faults in the Jurassic unit, our palinspastic reconstruction indicates that Jurassic beds have been shortened for ~21 km (42% strain), while the top of unit E1+2 has been shortened for ~40 km (53% strain).

Although the style of deformation in section (8) in the central segment of the North Qaidam thrust system resembles that in sections (1) to (3) in the western segment of the thrust system, the ages of the two structures are significantly different: the western triangle zone was initiated in the Paleocene-early Eocene, while the eastern triangle zone was initiated in the early Oligocene. This age difference suggests eastward younging of initiation of deformation along the northern margin of Qaidam basin, which was coeval with the southward propagation of deformation across the same region.

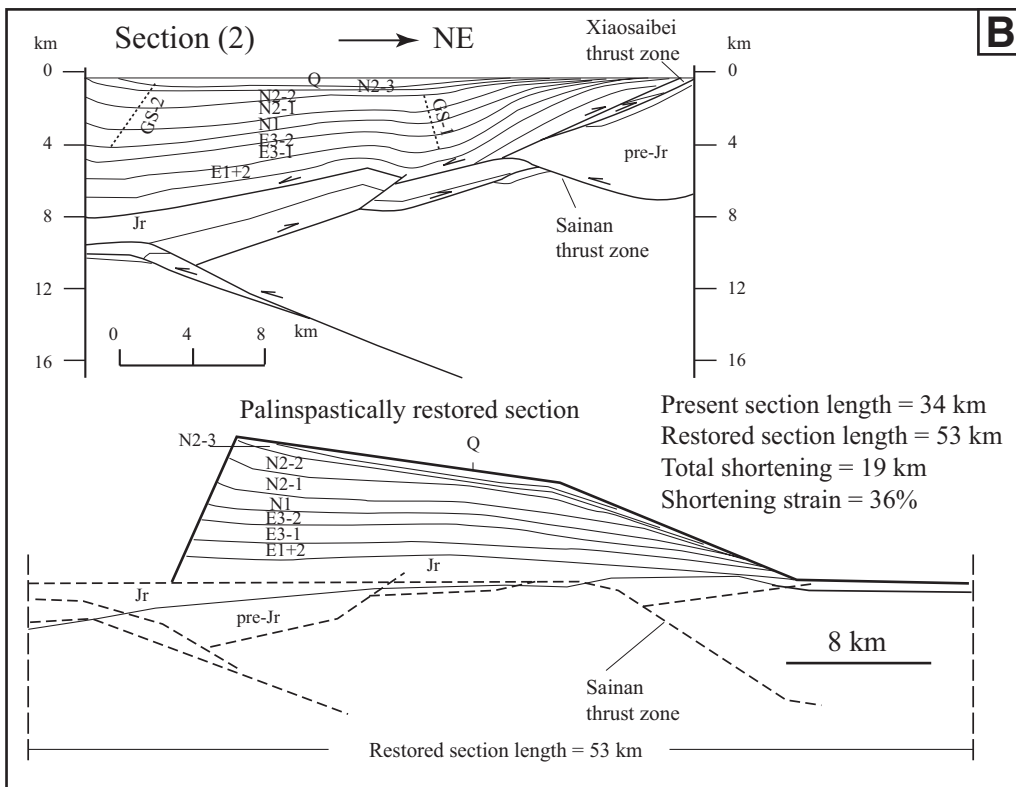
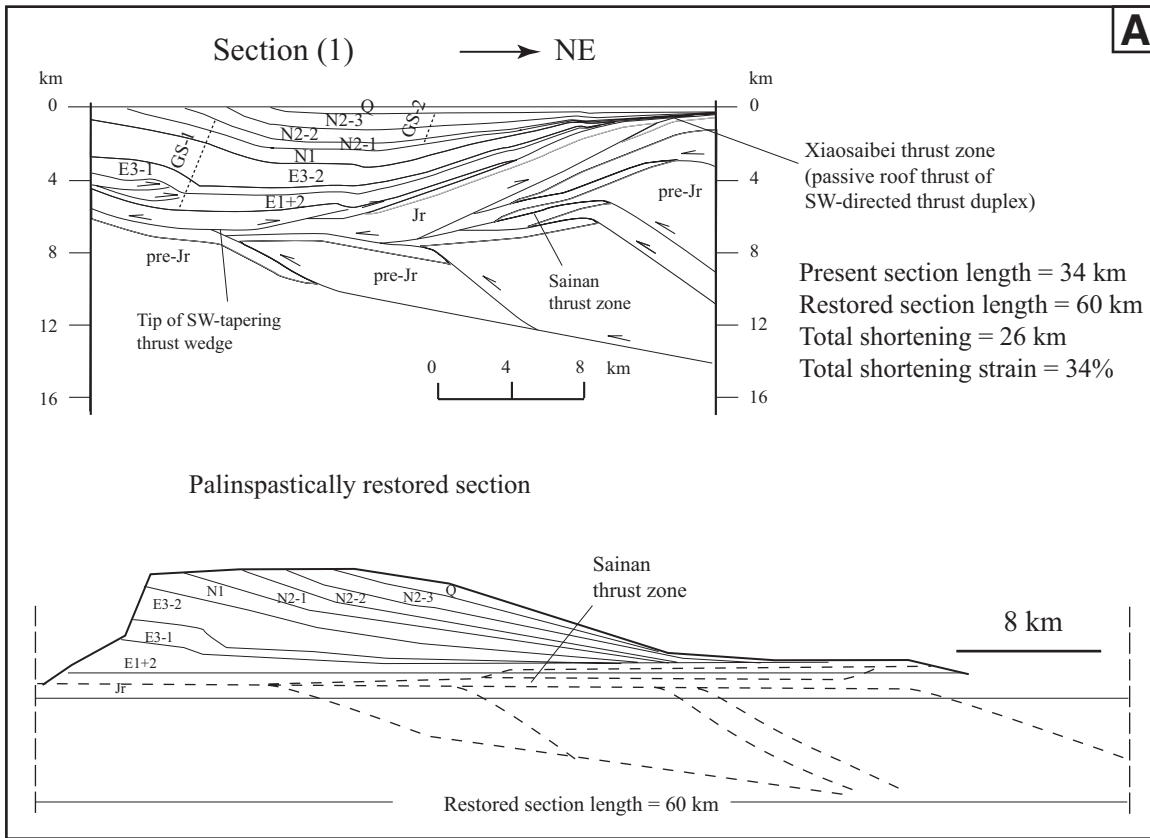


Figure 13. Interpreted seismic reflection profiles; see Figure 2 for locations. (A) Upper figure, geologic cross section interpreted from seismic profile (1). Lower figure, restored cross section. (B) Upper figure, geologic cross section interpreted from seismic profile (2). Lower figure, restored section. (Continued on following page.)

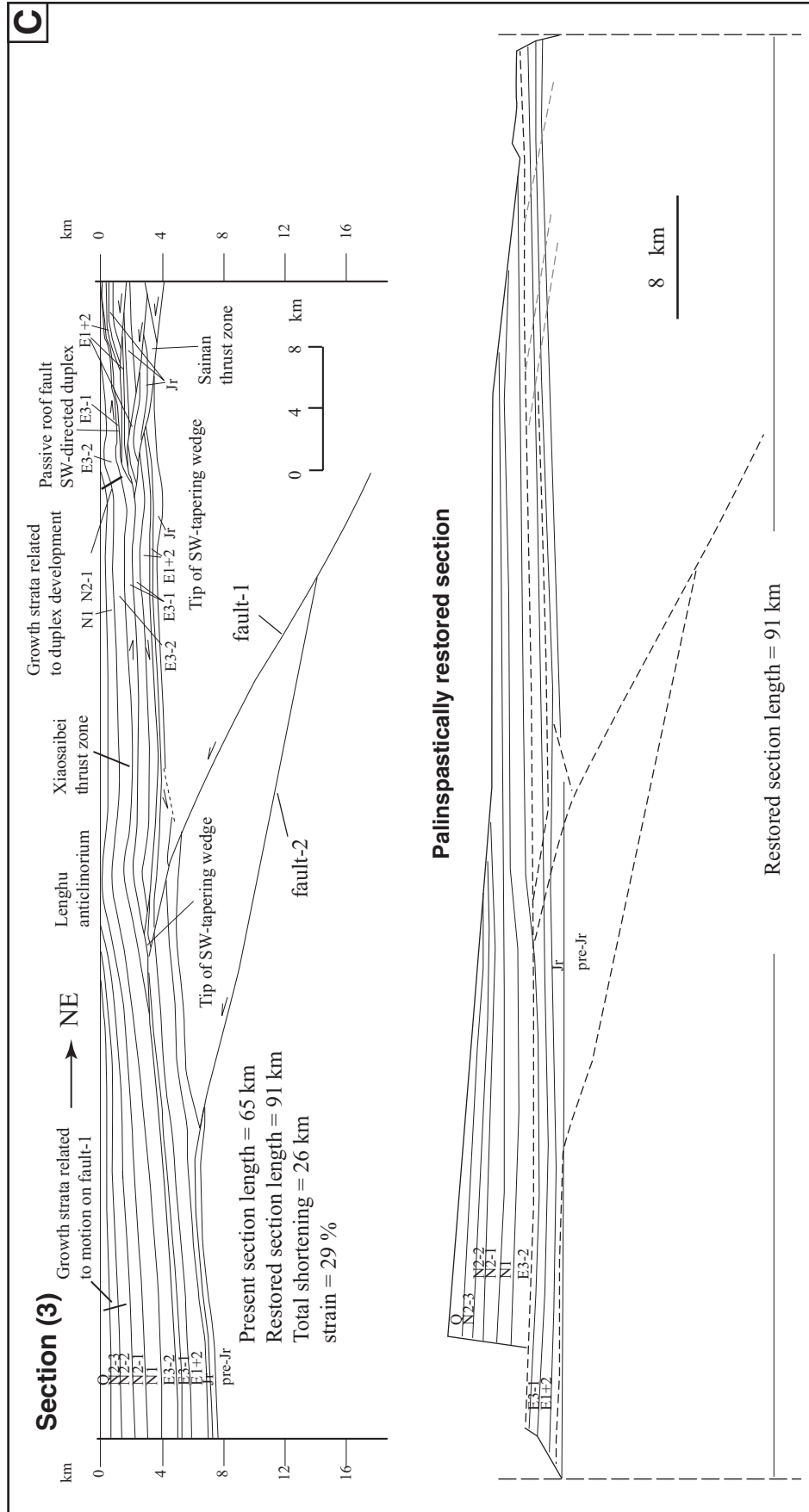


Figure 13 (continued). (C) Upper figure, geologic cross section interpreted from seismic profile (3). Lower figure, restored section.

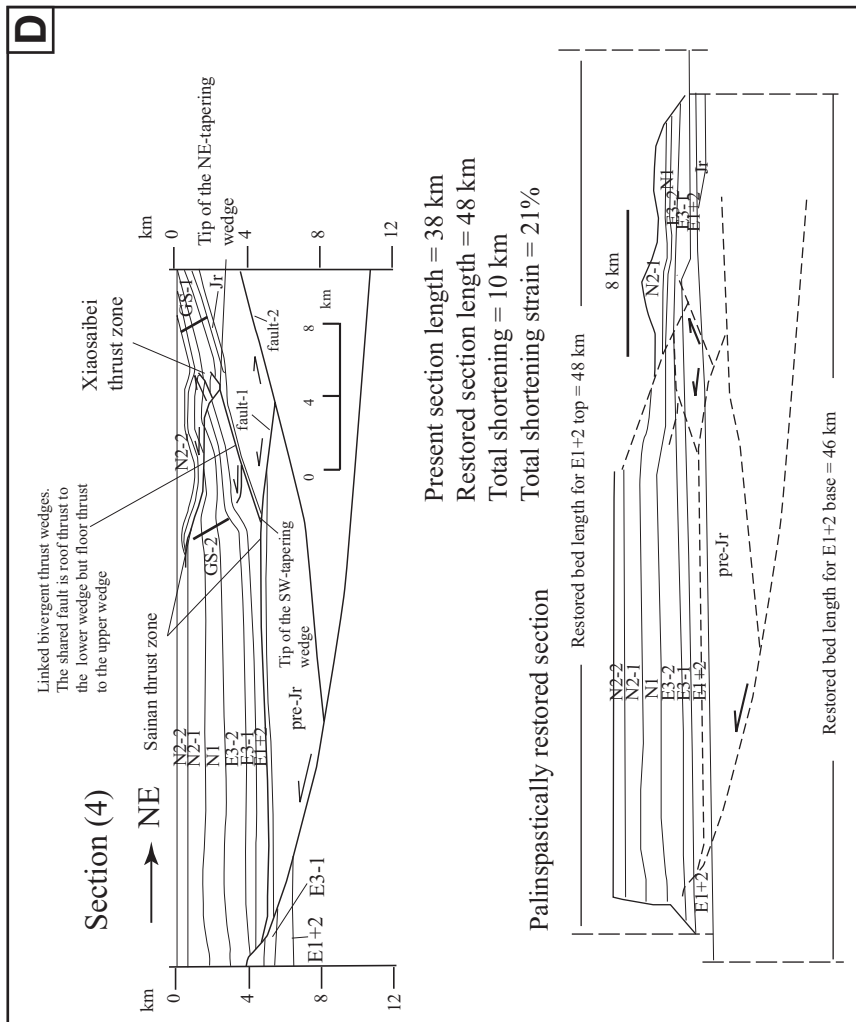
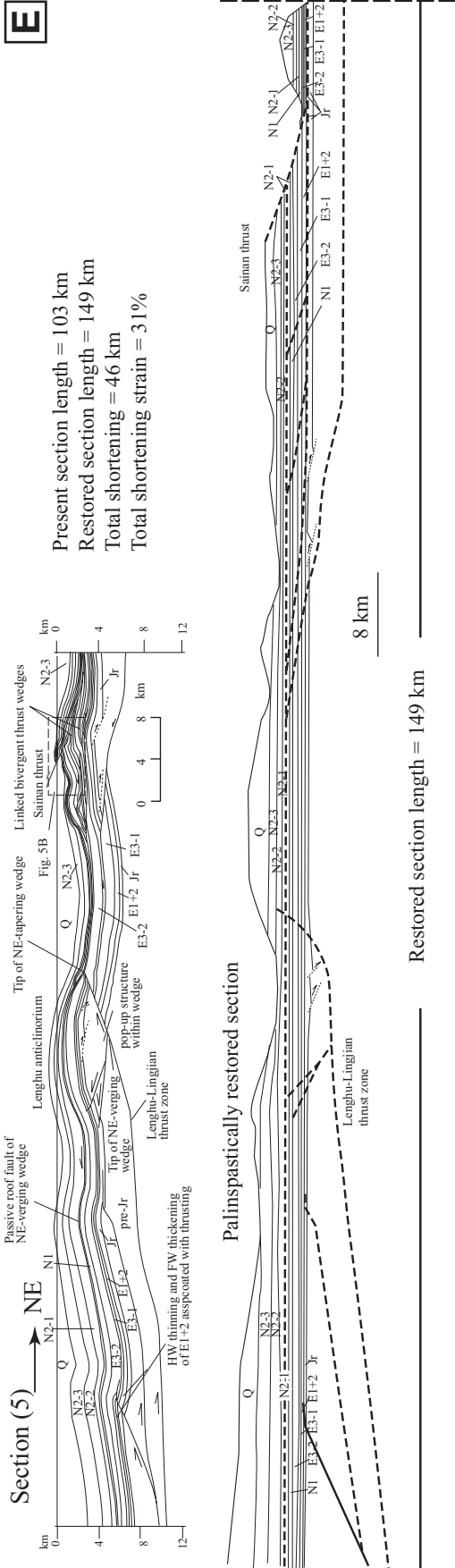


Figure 13 (continued). (D) Upper figure, geologic cross section interpreted from seismic profile (4). Lower figure, restored section. (Continued on following page.)

E



F

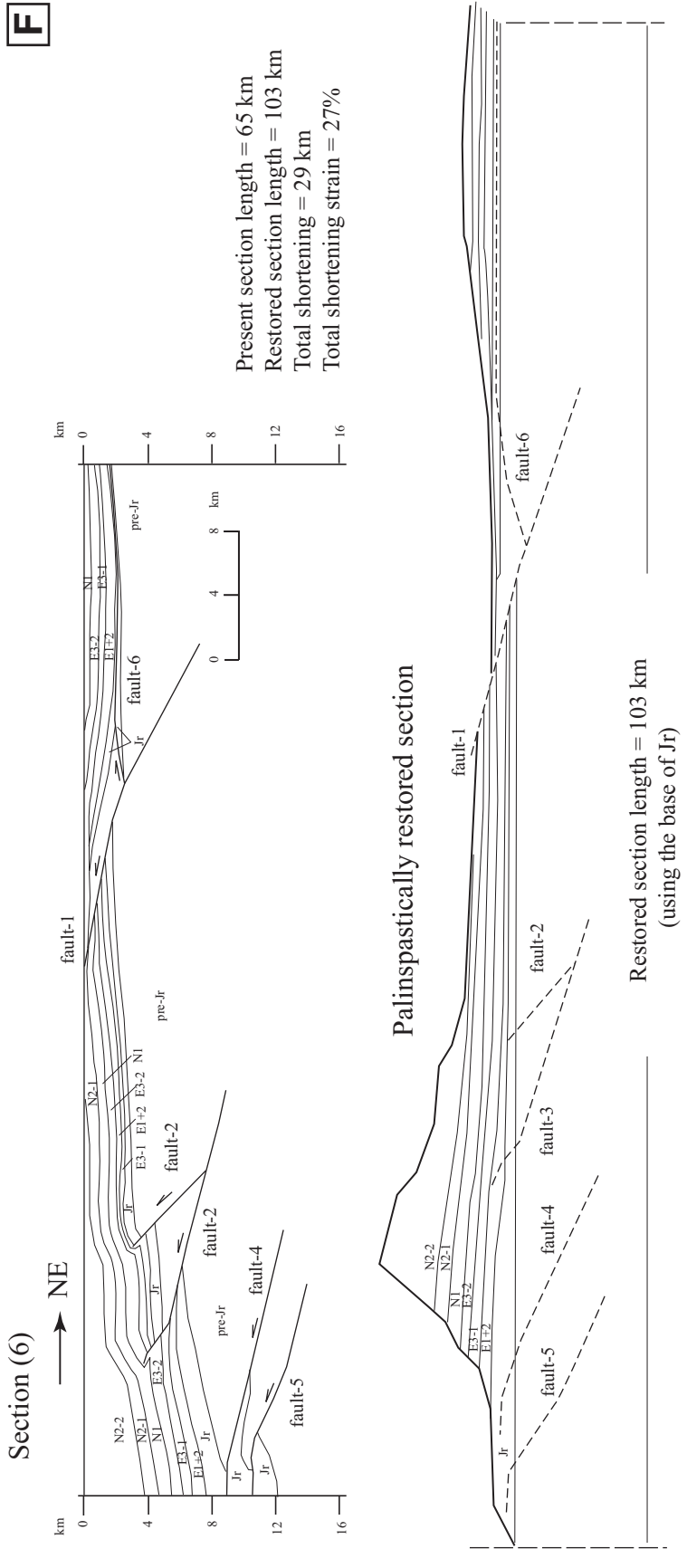


Figure 13 (continued). (E) Upper figure, geologic cross section interpreted from seismic profile (5). HW—Hanging Wall; FW—Footwall. Lower figure, restored section. (F) Upper geologic cross section interpreted from seismic profile (6). Lower figure, restored section. (Continued on following page.)

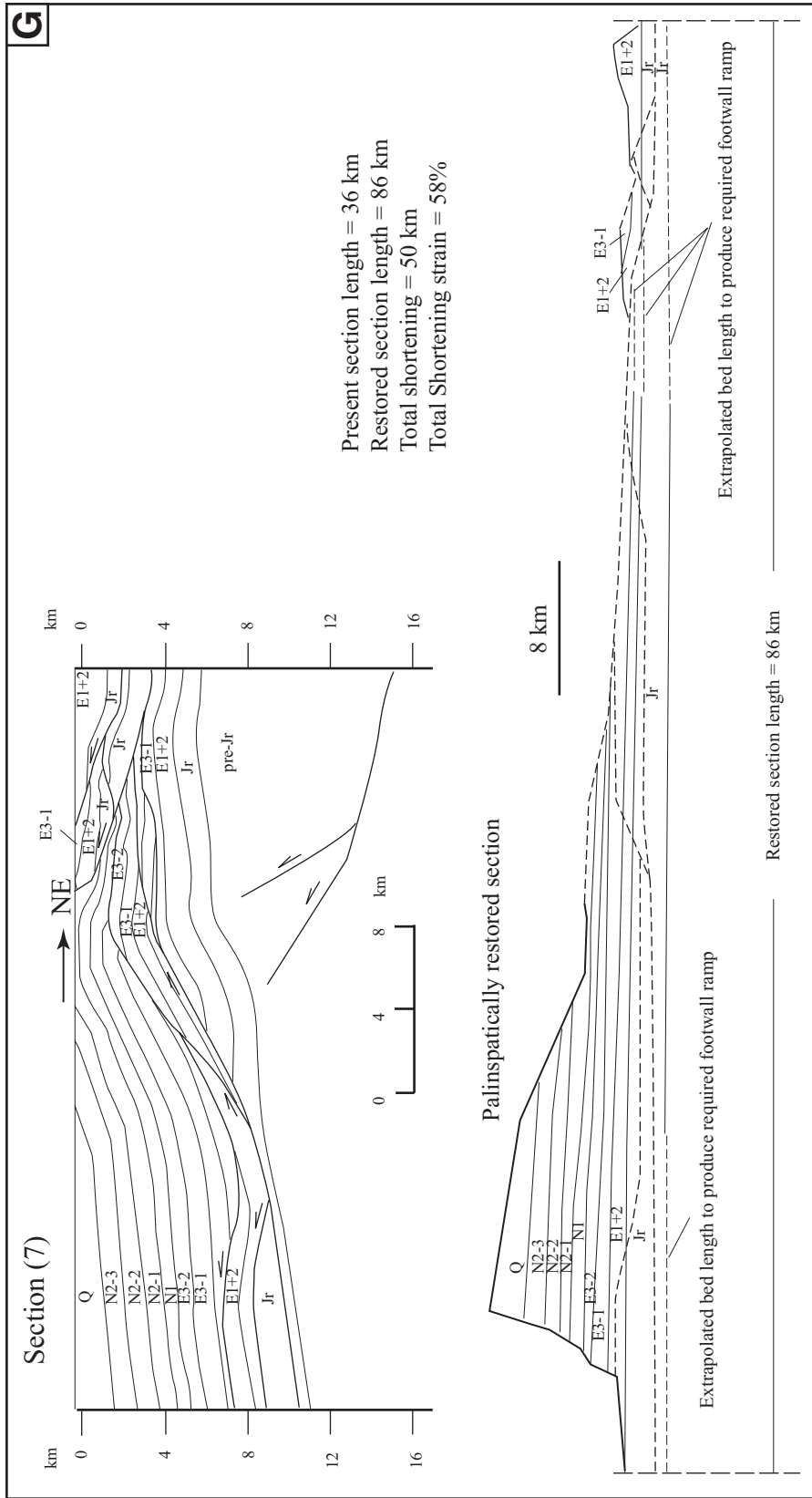


Figure 13 (continued). (G) Upper figure, geologic cross section interpreted from seismic profile (7). Lower figure, restored section. (Continued on following page.)

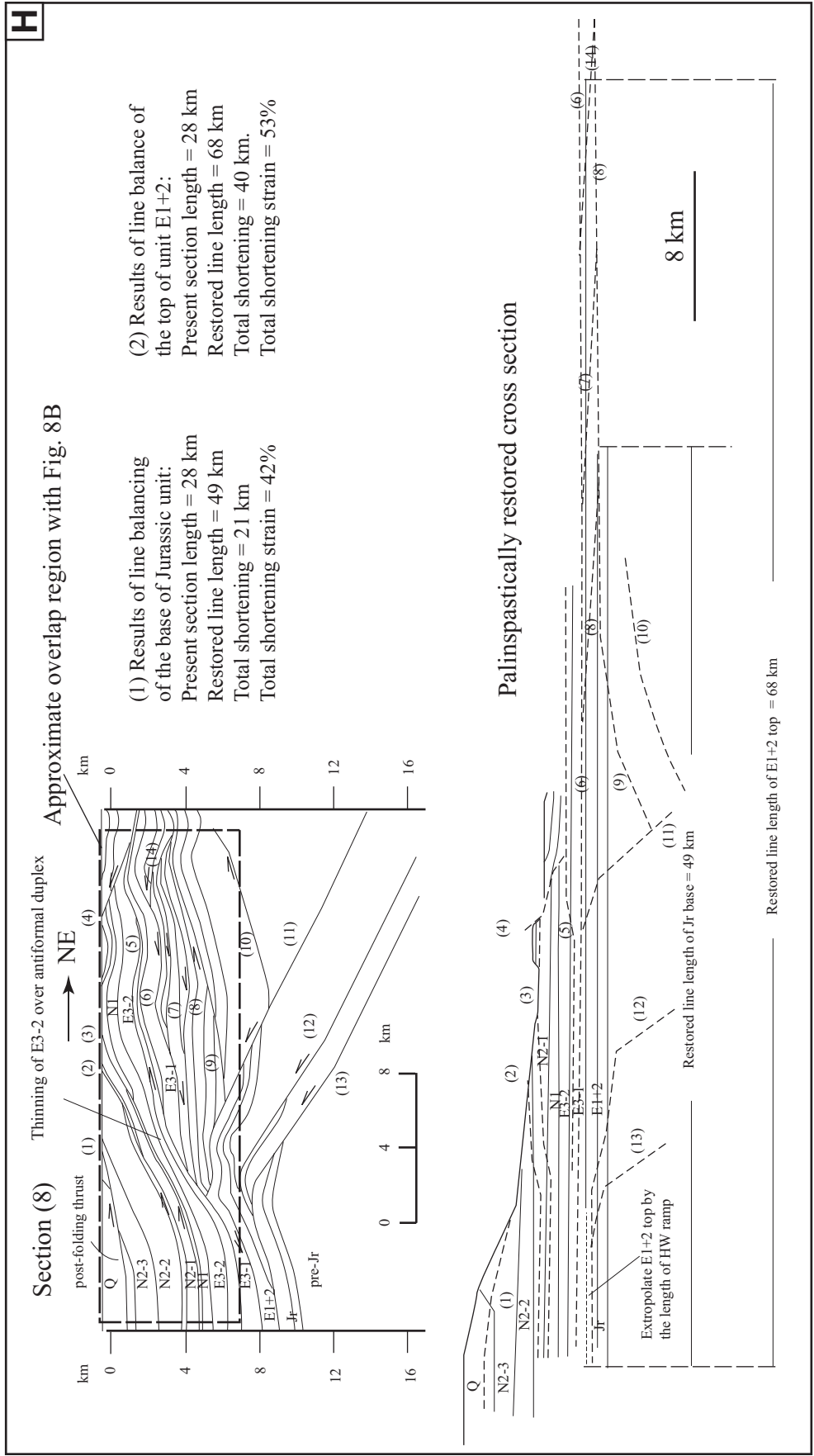


Figure 13 (continued). (H) Upper figure, geologic cross section interpreted from seismic profile (8). Lower figure, restored section. HW—Hanging Wall.

Because sections (7) and (8) cross the western part of our mapped area shown in Figure 8, we compare the overlapping segments of the cross sections constructed based on surface geology and seismic interpretations, respectively. In general, the style of deformation in the two cross sections is quite similar. However, the field-based cross section could not detect the complexly deformed thrust duplexes with multiple levels of bedding-parallel detachment horizons. Because of the presence of the bedding-parallel faults, the estimated shortening strain from surface geology (~23%) is much less than those estimated from seismic profiles (~53%–58%). We also note that fold amplitudes are much smaller and fold hinge zones are much broader in the seismic profile than those extrapolated from the surface geology guided by the dip-domain method.

KINEMATIC RECONSTRUCTION OF THE NORTH QAIDAM THRUST SYSTEM

Map-View Reconstruction

The growth-strata relationships in northern Qaidam basin indicate that Cenozoic deformation started first in the west against the left-slip Altyn Tagh fault and has subsequently propagated southward and eastward, respectively. Cenozoic deformation was initiated in the Paleocene and early Eocene in seismic sections (1) to (4) (Figs. 13A–13D), in the middle to late Eocene in seismic section (5) (Fig. 13E), and in the early Oligocene in section (8) (Fig. 13H). These observations yield an eastward-lengthening rate of ~8 km/m.y. for the North Qaidam thrust system. The southward propagation of deformation is best exemplified by the formation of the Lenghu anticlinorium currently lying within Qaidam basin. In contrast to southward propagation of deformation, out-of-sequence thrusting is documented in northern Qaidam basin as observed in seismic section (6) (Fig. 13F). In addition, some thrusts could have an extended dormant period (>20 m.y.) between two active periods (e.g., the Lenghu-Lingjian fault in Fig. 13E). These relationships suggest complex spatial and temporal evolution of contractional deformation across northern Qaidam basin.

Based on the above relationships, we reconstruct the development of the North Qaidam thrust system and associated sedimentation in Figure 14. To simplify the regional geology, we only consider major Cenozoic thrust zones discussed above (Figs. 2 and 14A). In the Paleocene and early Eocene, the Dasaibe thrust, Xiaosai-bei thrust, and Qaidam Shan thrust zone started to develop (Fig. 14B). This was associated with the development of a southwest-tapering thrust triangle zone along the northern margin of Qai-

dam basin and sedimentation of a southwestward thickening, growth-strata sequence across northern Qaidam basin.

The age of the Qaidam Shan thrust zone cannot be constrained from our own study. However, apatite fission-track work of Jolivet et al. (2001) provides the constraint, which shows that Luliang Shan gneiss in the footwall of the Qaidam Shan thrust experienced a reheating event at ca. 50 Ma (early to middle Eocene). These authors attributed the Eocene thermal event to deep burial either related to deposition of a thick Cenozoic sequence or thrusting of a thick hanging-wall section from above.

Farther to the southeast, the Sainan and Western Luliang Shan thrusts were initiated in the middle to late Eocene that were associated with deposition of unit E3–1 (Fig. 14C). This inference is based on the growth-strata and crosscutting relationships in the footwall of the Sainan thrust zone (Fig. 13E), although some of the thrusts in the Sainan thrust duplex to the northeast could have initiated earlier in the Paleocene and early Eocene. In the early Oligocene, the Eastern Luliang and Xitie Shan thrusts started to develop, during which unit E3–2 was deposited (Fig. 14D). This age inference is based on the growth-strata relationship in seismic profile (8) (Fig. 13H).

Between the late Oligocene and middle Miocene, deformation was mainly expressed by the development of the Lenghu anticlinorium as a result of southward propagation of deformation across northern Qaidam basin (Fig. 14E). From the late Miocene to Pliocene, the Aimunik-Olongbulak thrust system started to develop (Fig. 14F), producing growth strata along the southern flank of the Aimunik Shan (Fig. 4G). Southeastward expansion of Qaidam basin at this time is indicated by the unconformable relationship between the Neogene and Paleogene strata in the Xitie Shan in the west and the Neogene and pre-Cenozoic strata in the Aimunik Shan in the east (cf. Figs. 4G and 8). The eastward basin expansion at this time is also indicated by a rapid increase in sedimentation rate over the whole Qaidam basin (Huang et al., 1996; Métivier et al., 1998). Also during the late Miocene and Pliocene, contractional deformation propagated southward into the basin interior and created blind thrusts and related folds (Fig. 14F).

In the above reconstructions (Fig. 14), we hypothesize the presence of a series of south-flowing rivers carrying sediments from the Qilian Shan to the interior of Qaidam basin. The sediments were deposited in depocenters along the axis of the basin, which were deepened relatively to its surrounding mountain ranges due to the progressive development of the triangle zone along the basin margin. Also, the eastward

expansion of the North Qaidam thrust system was caused by sequential initiation of south-flowing river systems from the west to the east. This scenario explains both the eastward propagation of thrust deformation and the eastward expansion of Qaidam basin. We also envision that the south-flowing rivers were terminated into large playas, which is consistent with the fine-grained lacustrine deposition in central Qaidam basin since the early Oligocene (Huang et al., 1996; Zhang, 1997). The presence of the Oligocene to present lacustrine deposits in central Qaidam is inconsistent with the existence of a large longitudinal river as suggested by Wang et al. (2006).

Cross-Section Reconstruction

To better illustrate the structural evolution of the thrust triangle zone in northern Qaidam basin, we kinematically reconstructed seismic profiles (1) and (8) (Figs. 15A and 15B). For the development of profile (1), the triangle zone began to develop in the Paleocene to late Eocene (stage 2 in Fig. 15A). Its development produced a southwest-thickening, growth-strata sequence above a passive-roof duplex (stage 3 in Fig. 15A). This event was followed by continuous shortening of the duplex system from the late Oligocene to Pliocene, producing growth strata above (stage 4 in Fig. 15A). Finally, the older southwest-thickening, growth-strata sequence is folded. The later folding event created a younger Pliocene-Quaternary growth-strata sequence (stage 5 in Fig. 15A).

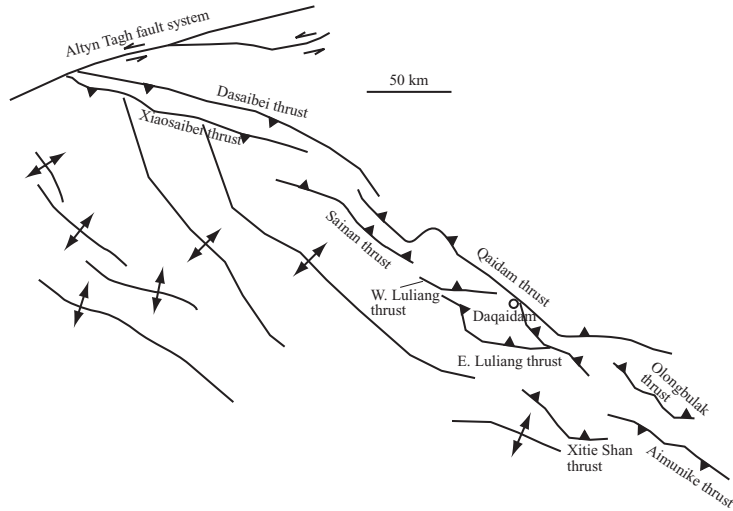
The kinematic reconstruction of seismic profile (8) (Fig. 13H) is shown in Figure 15B. The fault numbers in the reconstruction correspond to those shown in Figure 13H. From the growth-strata relationships, we interpret that the initiation of Cenozoic deformation occurred in the early Oligocene, which is significantly younger than the onset age of deformation in section (1) at the western end of the North Qaidam thrust system. The earliest Cenozoic deformation for section (8) was expressed by the development of a southwest-directed thrust duplex associated with deposition of an early Oligocene sequence above (stage 2 in Fig. 15A). This duplex system continued to develop in the Miocene (stages 2 and 3 in Fig. 15A) and was associated with the development of a break-back thrust (stage 4 in Fig. 15A). The final deformation was expressed by motion on two post-folding thrusts at the northern and southern ends of the section in the Pliocene and Quaternary (stages 5–7 in Fig. 15B).

DISCUSSION

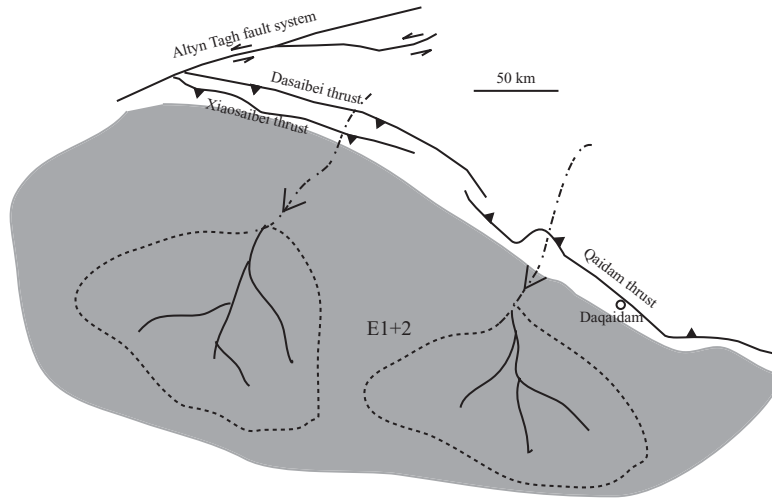
In map view, our study suggests that many thrusts in the southern Qilian Shan-Nan Shan

North Qaidam Basin

A
Present configuration
of North Qaidam thrust
system



B
Paleocene to early
Eocene (development
of Saibei, Lenghu, and
Qaidam thrusts)



C
Middle to late Eocene
(development of Sainan
and western Luliang
thrusts)

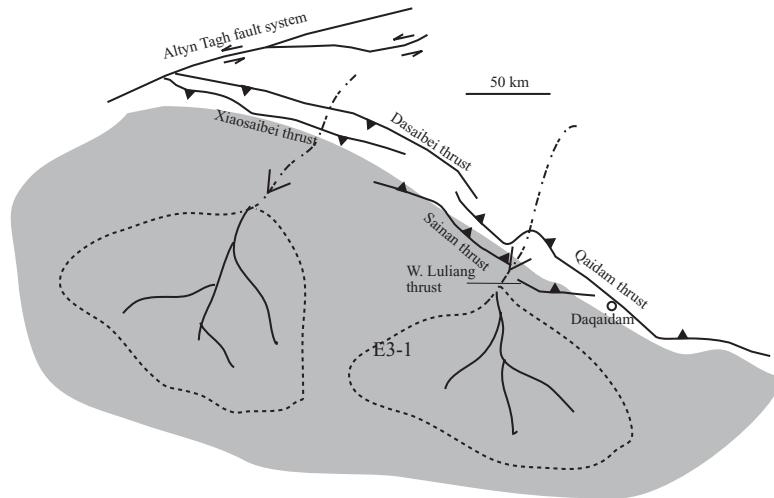
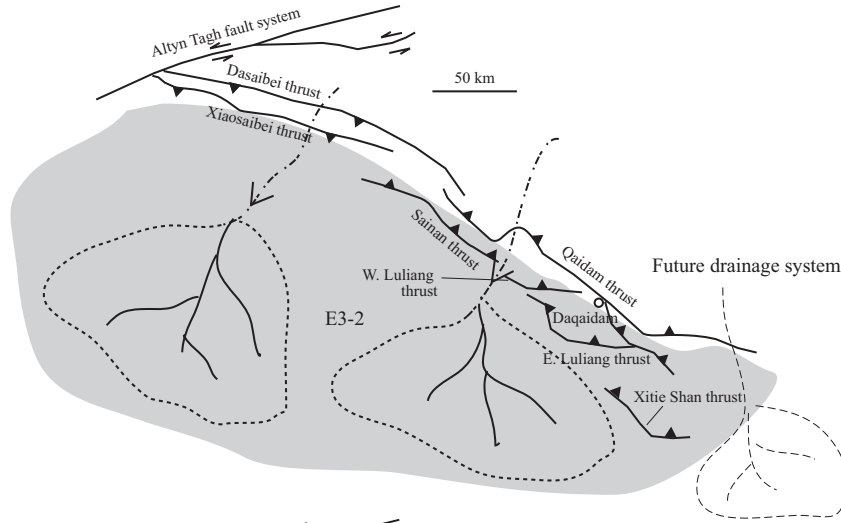


Figure 14. Tectonic evolution of the North Qaidam thrust system and depositional history of northern Qaidam basin. (A) Present tectonic configuration of the North Qaidam thrust belt. (B) Paleocene-early Eocene tectonic configuration of North Qaidam. (C) Middle to late Eocene tectonic configuration of North Qaidam. (D) Early Oligocene tectonic configuration of North Qaidam. (E) Late Oligocene to middle Miocene tectonic configuration of North Qaidam. (F) Late Miocene to Pliocene tectonic configuration of North Qaidam. (Continued on following page.)

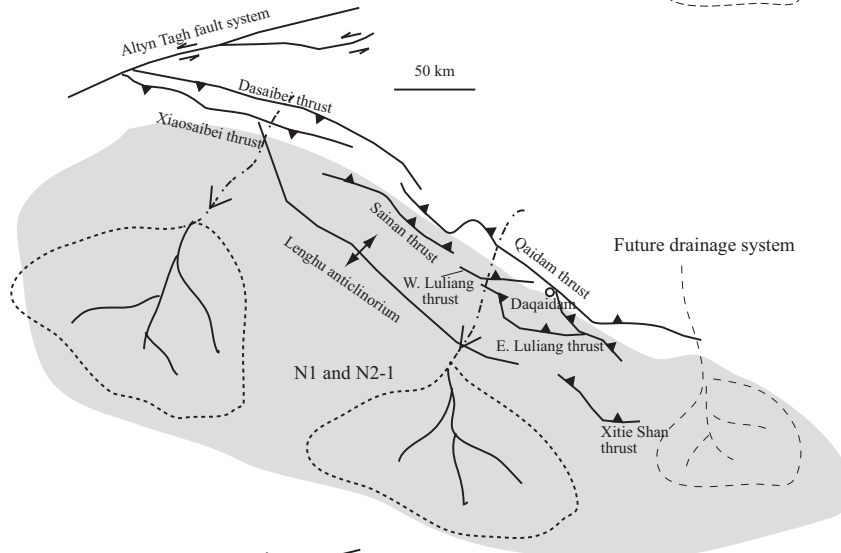
D

Early Oligocene (development of Eastern Luliang thrust and Xitie Shan thrust)



E

Late Oligocene to middle Miocene (development of Lenghu anticlinorium)



F

Late Miocene to Pliocene (development of Aimunike-Olongbulak thrust system and folds in central Qaidam)

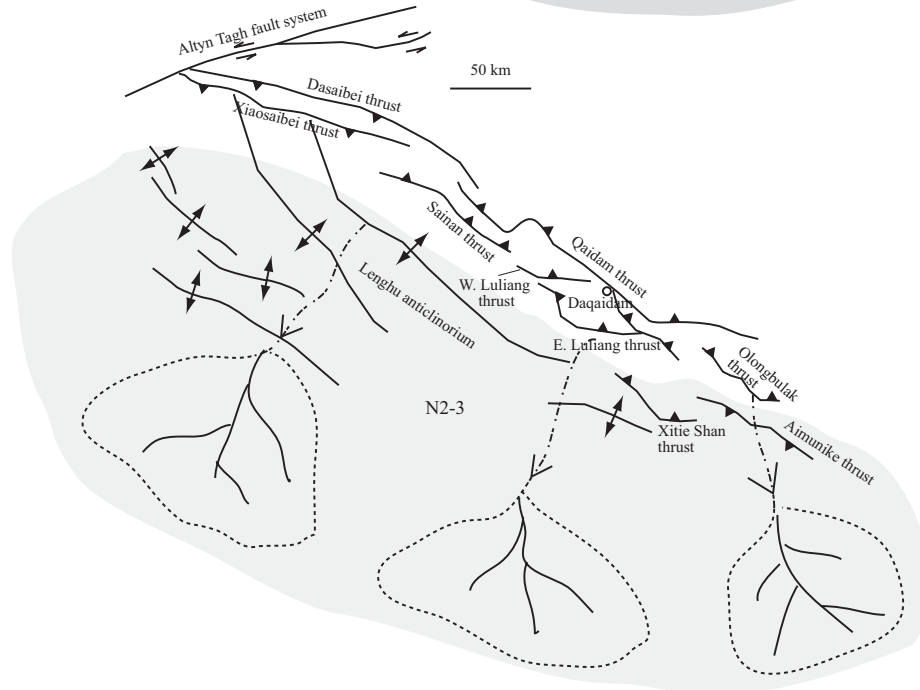


Figure 14 (continued)

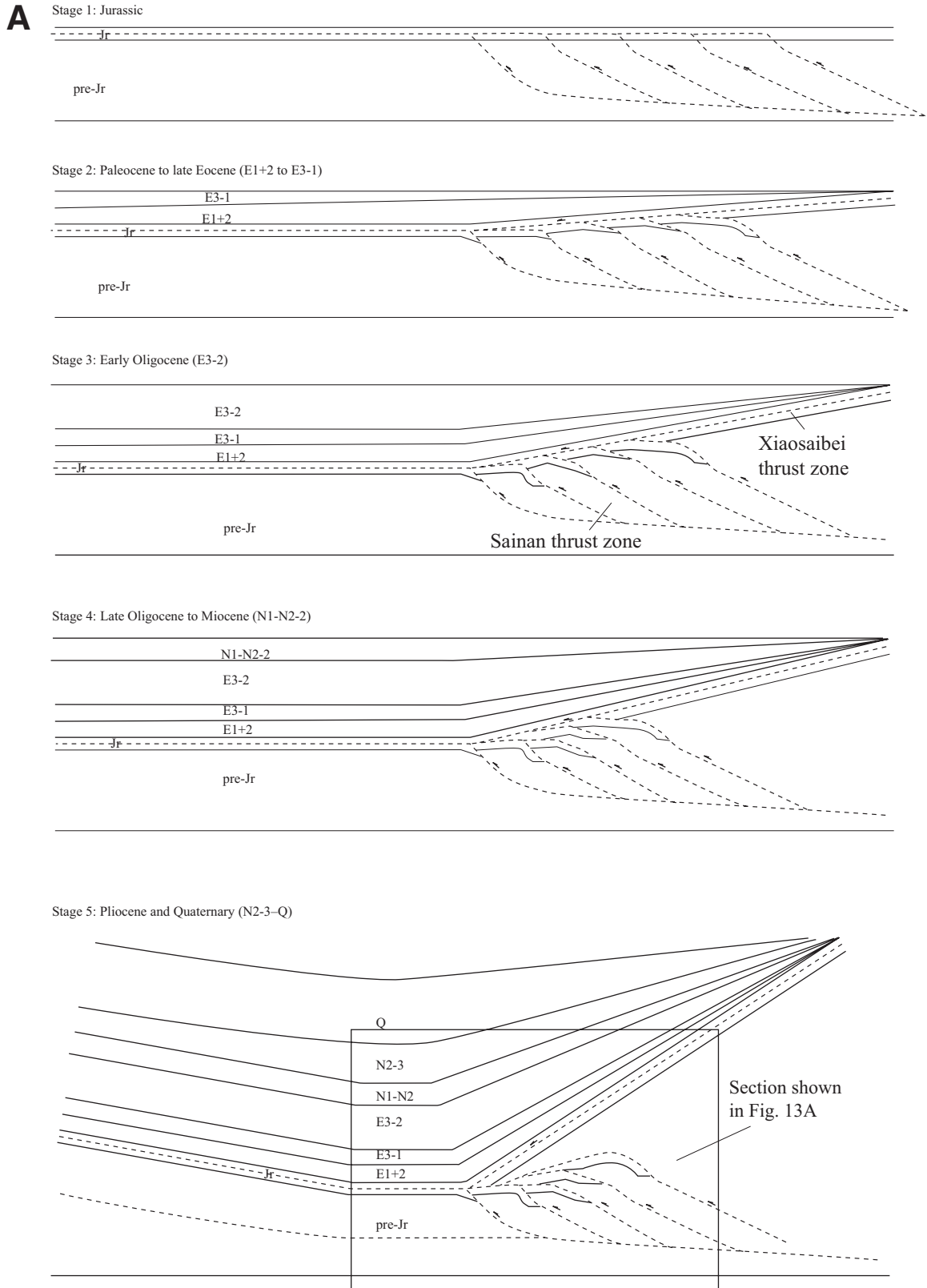


Figure 15. (A) Kinematic reconstruction of structural section shown in Figure 13A. See text for detailed description. (Continued on following page.)

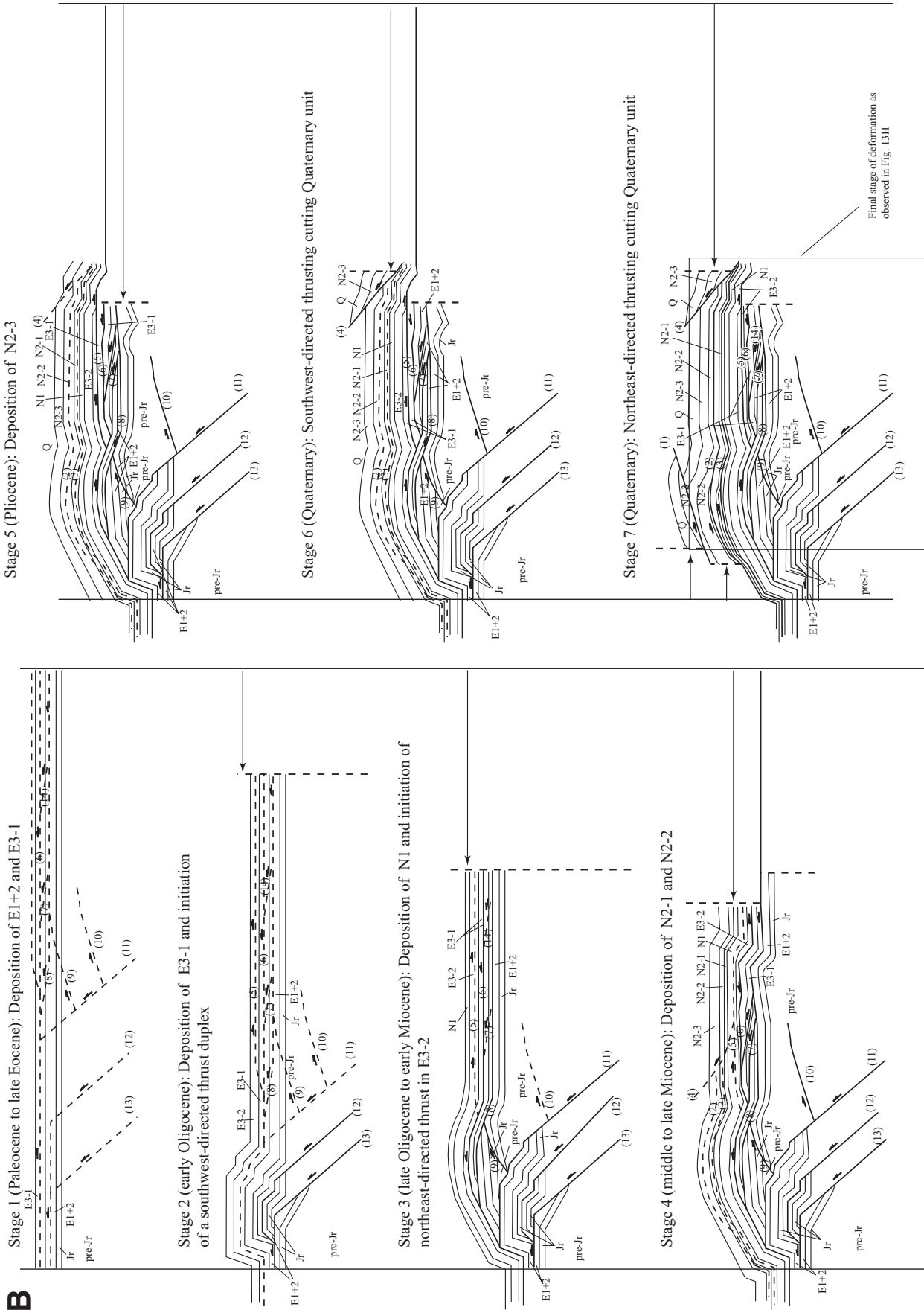


Figure 15 (continued). (B) Kinematic reconstruction of structural section shown in Figure 13H. See text for detailed description.

thrust belt and northern Qaidam basin exhibit L-shaped geometry, with the northwest-striking thrusts terminating in the west against the Altyn Tagh fault and in the east along east-striking, left-slip lateral ramps (Fig. 2). Because the lateral ramps are subparallel to the left-slip Altyn Tagh fault, their development may result from distributed left-slip deformation that transfers motion from the Altyn Tagh fault to the left-slip ramps via the linking thrusts. Such a mode of distributed left-slip deformation has not been recognized previously across northern Tibet.

In cross-section view, our interpreted seismic reflection profiles reveal complex structural associations in northern Qaidam basin that have accommodated a significant amount of crustal shortening (20% to >60%). The crustal shortening has been partitioned vertically through multi-story thrust wedges and duplex systems detached from weak stratigraphic horizons. This mode of deformation was anticipated by insightful analog experiments performed by Burg et al. (1994), which simulated possible crustal thickening processes during the development of the Tibetan plateau. Specifically, their experiments predict the development of bivergent thrust wedges that are common in the North Qaidam thrust system. Additionally, their experiments also predict nearly synchronous deformation across Tibet at the initial stage of the Indo-Asian collision, which is consistent with our observations.

Our geologic observations from northern Qaidam basin and the southern Qilian Shan-Nan Shan thrust belt also have important implications for how the Qaidam basin has developed and its relationship to the overall growth history of the Tibetan plateau. First, the discovery of a large triangle zone above a passive-roof duplex along the northern edge of Qaidam basin (Fig. 13) explains the observation that Cenozoic depocenters have been located consistently within rather than along the edge of the basin (Huang et al., 1996; Wang et al., 2006). This finding in a broad sense supports the early proposal by Bally et al. (1986) that Qaidam basin was created by the development of a large synclinorium rather than in a classic foreland basin setting (e.g., Jordan, 1981). The cause of the synclinorium was probably not induced by buckling under simple horizontal compression alone as envisioned by Burg et al. (1994). The fold development and its lateral expansion must have been accomplished by the development of multiple duplex systems at deeper crustal levels along the margins of Qaidam basin (also see Yin et al., 2008a). A well-documented example of a large synclinorium produced by duplex development is the folded Lewis thrust sheet in the southern Canadian Rocky Mountains and

western Montana of the United States (Price, 1981, 1986; Yin and Kelty, 1991).

Our study along the northern margin of the Qaidam basin cannot rule out the proposal that the basin originated from a trapping event due to a sudden northward jump of the northern plateau margin, because we do not have a solid constraint on the timing of structural development along the southern margin of Qaidam basin from this study (but see Yin et al., 2008b for discussion of this issue). However, if the trapping event did happen as the result of a jump of deformation front, it could not have developed in the Miocene-Pliocene as inferred by Meyer et al. (1998) and Métivier et al. (1998); such an age is too young to be consistent with the Paleocene and early Eocene initiation of the southern Qilian Shan-Nan Shan thrust belt as revealed by this study.

Our structural and sedimentological observations from northern Qaidam basin are consistent with the early suggestion that the basin has expanded eastward in the Cenozoic (Huang et al., 1996). Wang et al. (2006) suggested that the eastward expansion was induced by lateral extrusion of the northern Tibetan plateau and the development of an east-flowing longitudinal river system (the paleo-Kunlun River) along the axis of Qaidam basin. Specifically, their work in the southwestern part of Qaidam basin indicates that the eastward migration of the Qaidam depocenters between ca. 31 and 4 Ma was associated with thrusting and folding of the Cenozoic strata. This inference is broadly consistent with our observations across northern Qaidam basin, where eastward expansion of sedimentation corresponds temporally and spatially with nearby contractional structures. However, the presence of Oligocene to present lacustrine deposits in central Qaidam basin (Huang et al., 1996; Zhang, 1997) is not consistent with the existence of a paleo-longitudinal river along the basin axis as inferred by Wang et al. (2006).

The early Paleogene initiation of crustal shortening in northern Qaidam basin and the southern Qilian Shan-Nan Shan thrust belt is inconsistent with the prediction of the thin-viscous-sheet model, at least in its original form, which assumes uniform material properties across the whole Tibetan plateau (England and Houseman, 1986). This model predicts progressive and continuous northward enlargement of the Tibetan plateau and implies crustal shortening in the Qilian Shan-Nan Shan region to have started in the last stage, rather than at the onset, of the Indo-Asian collision. A revised thin-viscous-sheet model considering heterogeneous mechanical strength, preexisting weakness, and preexisting topography in Asian lithosphere prior to the Indo-Asian collision better explains

the complex Cenozoic deformation history across Tibet and Asia in general (e.g., Neil and Houseman, 1997; Kong et al., 1997). Paleocene-early Eocene initiation of contractional deformation in northern Qaidam basin is consistent with other studies that indicate Eocene initiation of deformation along the present northern margin of the Tibetan plateau (Yin et al., 2002; Dupont-Nivet et al., 2004; Horton et al., 2004). Together, these studies require rapid and efficient stress transfer from the convergent front of the Indo-Asian collision zone in the south to the interior of the Asian continent >1000 km in the north during the early stage of the continental collision (e.g., Burg et al., 1994).

Although it has long been recognized that the Cenozoic contractional structures in the Qilian Shan-Nan Shan thrust belt are geometrically and kinematically linked with the Altyn Tagh fault (Bally et al., 1986; Burchfiel et al., 1989; Tapponnier et al., 1990), their temporal relationships are only locally known and mostly along the Altyn Tagh fault zone (e.g., Bally et al., 1986; Wang, 1997; Hanson, 1998; Yin et al., 2002; Wang et al., 2006). The results of our study provide new insight into this issue. In the previous studies, several authors have inferred that individual rows of northwest-trending thrust systems in the Qilian Shan-Nan Shan thrust belt were initiated simultaneously along strike, with the thrust front migrating progressively to the north (e.g., Wang, 1997; Meyer et al., 1998; Yin et al., 2002). The observations from this study suggest that it may take tens of millions of years for individual rows of thrust systems to propagate laterally from the western end to the eastern end of the Qilian Shan-Nan Shan thrust belt. Our observations across northern Qaidam basin also imply that the growth of the Tibetan plateau was closely related to motion on the Altyn Tagh fault; that is, slip on the fault has driven crustal shortening across northern Tibet (Burchfiel et al., 1989; Tapponnier et al., 1990; Meyer et al., 1998).

Determining the magnitude of Cenozoic shortening is a key to evaluating whether lower-crustal flow or thermal events in the mantle were responsible for the uplift of the Tibetan plateau (Clark and Royden, 2000; Molnar et al., 1993). Among the thirteen structural sections we examined, five record shortening strain >50%, five record strain between 30% and 39%, and three record strain between 20% and 29%. If the entire crust has been deformed by pure-shear shortening in the Cenozoic, our estimated shortening strain on average is more than sufficient to explain the present elevation (3000–3500 m) and crustal thickness (45–50 km) of the northern Qaidam region, because thickening a crust from 35 km to 45–50 km requires a shortening

strain of 29%–42%. If Cenozoic deformation in the upper and lower crust was decoupled by a detachment (Burchfiel et al., 1989), then the overall Cenozoic shortening strain may be partitioned vertically in a more complex way. For example, it is possible that our observed upper crustal shortening represents pure-shear contraction above the inferred mid-crustal detachment; meanwhile the lower crust of Qaidam basin has undergone a combined pure- and simple-shear deformation (i.e., general shear) accommodating both crustal thickening and northeastward subduction of the Qaidam mantle lithosphere below the Qilian Shan-Nan Shan thrust belt (Fig. 16). Testing this more complex scenario requires the knowledge of lithospheric-scale structures across the region, which is clearly beyond the scope of this study.

As mentioned above, the magnitude of Cenozoic rotation varies spatially across Qaidam basin (Dupont-Nivet et al., 2002; Chen et al., 2002; Halim et al., 2003; Sun et al., 2006). Our observed inhomogeneous strain distribution across northern Qaidam basin, rapid lateral termination of contractional structures from thrusts to folds, and the presence of lateral ramps and

younger strike-slip faults could all help explain these conflicting results. It will be a fruitful research area in the future to quantitatively correlate the timing and magnitude of local Cenozoic rotation with the evolution of individual structures in cross-section and map views.

Although it was not the main emphasis of this study, seismic profiles have also provided new insights into the Jurassic and Cretaceous tectonic setting across the Qaidam region. The Qaidam region in the Jurassic has been regarded as a single, large foreland basin in front of a north-directed thrust belt in the Eastern Kunlun Shan to the south (Ritts and Biffi, 2000). The single-basin conceptual model was used as a guide to constrain the magnitude of offset across the Altyn Tagh fault by matching possible lake shorelines (Ritts and Biffi, 2000). As indicated by surface mapping and the analysis of seismic data, the central and northern Tibetan plateau (including the Qaidam basin) in the Jurassic and Cretaceous had experienced several phases of extension (Huo and Tan, 1995; Huang et al., 1996; Sobel, 1999; Vincent and Allen, 1999; Kapp et al., 2000, 2003; Xia et al., 2001; Chen et al., 2003; Horton et al., 2004). Specifically,

the Qaidam region in Jurassic time consists of several isolated basins (Huang et al., 1996; Xia et al., 2001), which would make the correlation of lake shorelines highly nonunique across the Cenozoic Altyn Tagh fault (i.e., slip across the Altyn Tagh fault could be significantly larger or smaller than that estimated by Ritts and Biffi, 2000). This uncertainty should be kept in mind in any tectonic reconstruction of the Tibetan plateau in the future.

CONCLUSIONS

New structural observations from the southern Qilian Shan-Nan Shan thrust belt and northern Qaidam basin allow us to evaluate the timing and magnitude of Cenozoic deformation. In this study, we show that the southernmost part of the Qilian Shan-Nan Shan thrust belt and contractional structures along the northern margin of Qaidam basin were initiated in the Paleocene-early Eocene (65–50 Ma) during or immediately after the onset of the Indo-Asian collision. This finding implies that stress was transferred rapidly and effectively across Tibetan lithosphere to its northern margin over a distance of

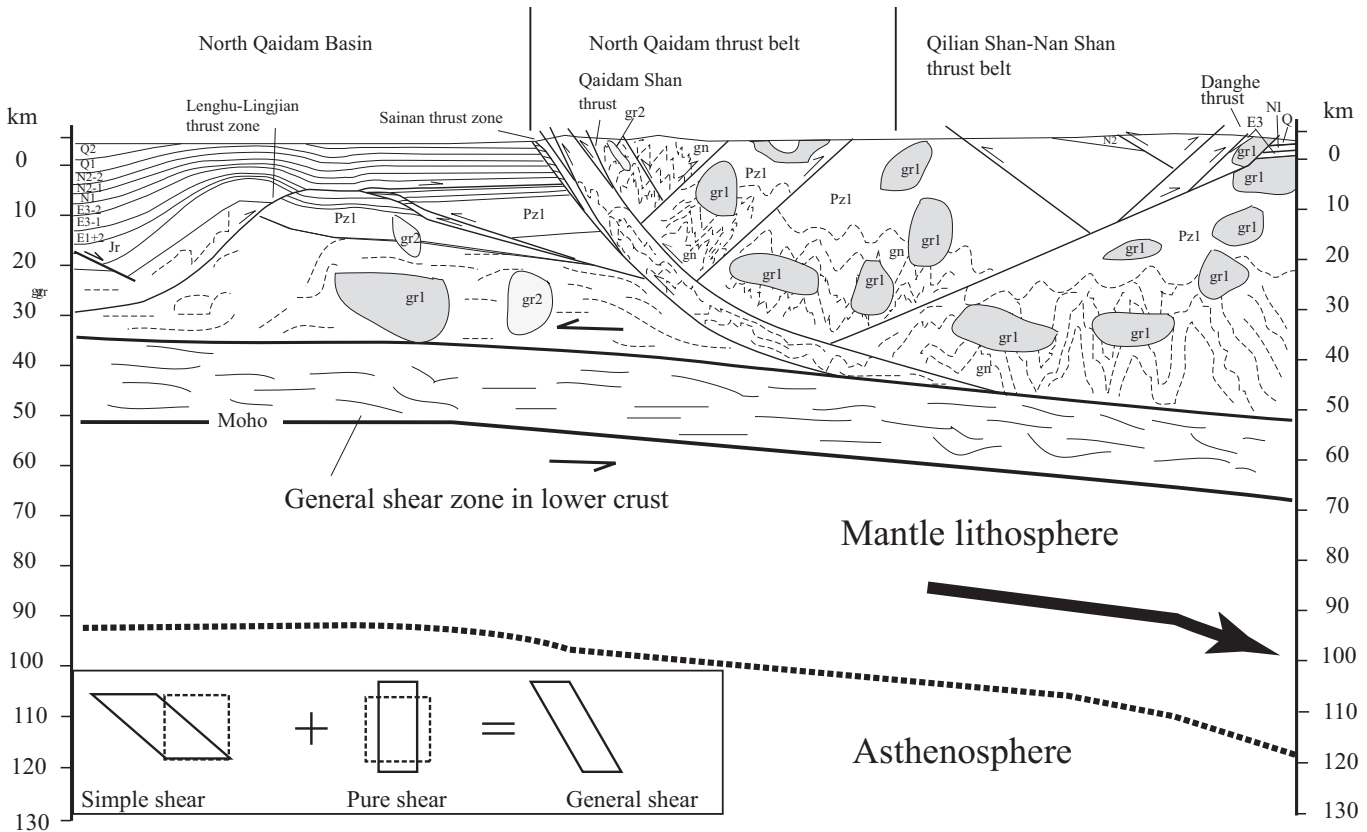


Figure 16. Schematic regional geologic cross section across the southern Qilian Shan-Nan Shan thrust belt and northern Qaidam; see Figure 2 for location. The geology of northern Qaidam basin is based on interpretation of seismic reflection profiles. Lower crust in northern Qaidam basin may have undergone general shear deformation, accommodating both vertical crustal thickening and top-southwest simple shear.

>1000 km from the Indo-Asian convergent front to the south. The North Qaidam thrust system is dominated by southwest-directed thrusts with a southwest-tapering thrust wedge (i.e., the triangle zone). The recognition of the triangle zone and its longevity in northern Qaidam basin explain a long puzzling observation that Cenozoic depocenters have been located consistently along the central axis of the basin, which is opposite to the prediction of a classic foreland-basin model requiring the thickest part of foreland sediments to lie along the basin edges directly against the bounding thrust belt. Restoring balanced cross sections across the southern Qilian Shan-Nan Shan thrust belt and northern Qaidam basin suggests that the Cenozoic shortening strain is highly inhomogeneous, varying from ~20% to >60%. However, the averaged shortening strain across northern Qaidam basin is sufficient to explain the Cenozoic shortening strain of ~20% to >60%, which also implies that no lower-crustal injection or thermal event in the mantle are needed to explain the current elevation (~3000–3500 m) and crustal thickness (45–50 km) of the region. The spatial variable strain also helps explain the conflicting paleomagnetic results indicating different magnitudes of Cenozoic rotation across Qaidam basin.

ACKNOWLEDGMENTS

We thank J.-P. Burg and Ray Price for their excellent reviews. Ray Price's insightful comments on thrust geometry and cross-section balancing led to significant revision of the original text. We also thank Associate Editor Laurent Godin and Science Editor Brendan Murphy for their constructive suggestions. Their comments have helped improve greatly the original manuscript. An Yin's research in Tibet was supported by the U.S. National Science Foundation. Research on this project would not be possible without the support of the Qinghai Oilfield Company of PetroChina and the China University of Geosciences (Beijing). The research was mostly conducted while the first author was a summer visiting professor at the China University of Geosciences, which was sponsored by the Chinese Ministry of Education via a Changjiang Visiting Professor Fellowship.

REFERENCES CITED

- Bally, A.W., Chou, I.-M., Clayton, R., Eugster, H.P., Kidwell, S., Meckel, L.D., Ryder, R.T., Watts, A.B., and Wilson, A.A., 1986, Notes on sedimentary basins in China—Report of the American sedimentary basins delegation to the People's Republic of China: U.S. Geological Survey Open-File Report 86-327, 108 p.
- Braitenberg, C., Wang, Y., Fang, J., and Hsu, H.T., 2003, Spatial variations of flexure parameters over the Tibet-Qinghai plateau: Earth and Planetary Science Letters, v. 205, p. 211–224, doi: 10.1016/S0012-821X(02)01042-7.
- Burchfiel, B.C., and Royden, L.H., 1991, Tectonics of Asia 50 years after the death of Emile Argand: *Eclogae Geologicae Helveticae*, v. 84, p. 599–629.
- Burchfiel, B.C., Deng, Q., Molnar, P., Royden, L.H., Wang, Y., Zhang, P., and Zhang, W., 1989, Intracrustal detachment with zones of continental deformation: *Geology*, v. 17, p. 748–752, doi: 10.1130/0091-7613(1989)017<0448:IDWZOC>2.3.CO;2.
- Burg, J.P., Davy, P., and Martinod, J., 1994, Shortening of analog models of the continental lithosphere—New hypothesis for the formation of the Tibetan plateau: *Tectonics*, v. 13, p. 475–483, doi: 10.1029/93TC02738.
- Chen, X.H., Yin, A., Gehrels, G.E., Cowgill, E., Grove, M., Harrison, T.M., and Wang, X.F., 2003, Two phases of Mesozoic north-south extension in the eastern Altyn Tagh Range, northern Tibetan plateau: *Tectonics*, v. 22, p. 1053, doi: 10.1029/2001TC001336.
- Chen, Y., Gilder, S., Halim, N., Cogne, J.P., and Courtillot, V., 2002, New paleomagnetic constraints on central Asian kinematics: Displacement along the Altyn Tagh fault and rotation of the Qaidam Basin: *Tectonics*, v. 21, Art. No. 1042.
- Clark, M.K., and Royden, L.H., 2000, Topographic ooze: Building the eastern margin of Tibet by lower crustal flow: *Geology*, v. 28, p. 703–706, doi: 10.1130/0091-7613(2000)28<703:TOBTEM>2.0.CO;2.
- Dang, Y., Hu, Y., Yu, H., Song, Y., and Yang, F., 2003, Petroleum geology of northern Qaidam basin: Beijing, Geological Publishing House, 187 p.
- DeCelles, P.G., Robinson, D.M., and Zandt, G., 2002, Implications of shortening in the Himalayan fold-thrust belt for uplift of the Tibetan Plateau: *Tectonics*, v. 21, p. 1062, doi: 10.1029/2001TC001322.
- Dewey, J.F., Shackleton, R.M., Chang, C., and Sun, Y., 1988, The tectonic evolution of the Tibetan Plateau: *Philosophical Transactions of the Royal Society of London, Series A*, v. 327, p. 379–413, doi: 10.1098/rsta.1988.0135.
- Dupont-Nivet, G., Butler, R.F., Yin, A., and Chen, X., 2002, Paleomagnetism indicates no Neogene rotation of Qaidam basin in northern Tibet during Indo-Asian collision: *Geology*, v. 30, p. 263–266, doi: 10.1130/0091-7613(2002)030<0263:PINNRO>2.0.CO;2.
- Dupont-Nivet, G., Horton, B.K., Butler, R.F., Wang, J., Zhou, J., and Waanders, G.L., 2004, Paleogene clockwise tectonic rotation of the Xining-Lanzhou region, northeastern Tibetan Plateau: *Journal of Geophysical Research*, v. 109, p. B04401, doi: 10.1029/2003JB002620.
- England, P., and Houseman, G., 1986, Finite strain calculations of continental deformation: 2. Comparison with the India-Asia collision zone: *Journal of Geophysical Research*, v. 91, p. 3664–3676.
- England, P., and Houseman, G., 1989, Extension during continental convergence, with application to the Tibetan Plateau: *Journal of Geophysical Research*, v. 94, p. 17,561–17,569.
- Gehrels, G.E., Yin, A., and Wang, X.F., 2003a, Detrital zircon geochronology of the northeastern Tibet: *Geological Society of America Bulletin*, v. 115, p. 881–896, doi: 10.1130/0016-7606(2003)115<0881:DGOTNT>2.0.CO;2.
- Gehrels, G.E., Yin, A., and Wang, X.F., 2003b, Magmatic history of the Altyn Tagh, Nan Shan, and Qilian Shan region of western China: *Journal of Geophysical Research*, v. 108, p. 2423, doi: 10.1029/2002JB001876.
- Guo, Z.J., Zhang, Z.C., and Wang, J.J., 1999, Sm-Nd isochron age of ophiolite along northern margin of Altun Tagh Mountain and its tectonic significance: *Chinese Science Bulletin*, v. 44, p. 456–458.
- Halim, N., Chen, Y., and Cogne, J.P., 2003, A first palaeomagnetic study of Jurassic formations from the Qaidam basin, Northeastern Tibet, China—Tectonic implications: *Geophysical Journal International*, v. 153, p. 20–26, doi: 10.1046/j.1365-246X.2003.01860.x.
- Hanson, A.D., 1998, Orogenic geochemistry and petroleum geology, tectonics and basin analysis of southern Tarim and northern Qaidam basins, northwest China [Ph.D. thesis]: Stanford University, p. 316.
- Harrison, T.M., Copeland, P., Kidd, W.S.F., and Yin, A., 1992, Raising Tibet: *Science*, v. 255, p. 1663–1670, doi: 10.1126/science.255.5052.1663.
- Horton, B.K., Dupont-Nivet, G., Zhou, J., Waanders, G.L., Butler, R.F., and Wang, J., 2004, Mesozoic-Cenozoic evolution of the Xining-Minhe and Dangchang basins, northeastern Tibetan Plateau magnetostratigraphic and biostratigraphic results: *Journal of Geophysical Research*, v. 109, p. B04402, doi: 10.1029/2003JB002913.
- Huang, H., Huang, Q., and Ma, Y., 1996, Geology of Qaidam basin and its petroleum prediction: Beijing, Geological Publishing House.

- Huo, G.M., ed., 1990, Petroleum geology of China: Oil fields in Qianghai and Xizang: Chinese Petroleum Industry Press, v. 14, 483 p.
- Huo, Y.L., and Tan, S.D., 1995, Exploration case history and petroleum geology in Jiuquan continental basin: Beijing, Petroleum Industry Press, 211 p.
- Jolivet, M., Brunel, M., Seward, D., Xu, Z., Yang, J., Roger, F., Tapponnier, P., Malavieille, J., Arnaud, N., and Wu, C., 2001, Mesozoic and Cenozoic tectonics of the northern edge of the Tibetan plateau: Fission-track constraints: *Tectonophysics*, v. 343, p. 111–134, doi: 10.1016/S0040-1951(01)00196-2.
- Jordan, T.E., 1981, Thrust loads and foreland basin evolution, Cretaceous, western United States: *American Association of Petroleum Geologists Bulletin*, v. 65, p. 2506–2520.
- Kapp, P.P., Yin, A., Manning, C., Murphy, M.A., Harrison, T.M., Ding, L., Deng, X.G., and Wu, C.-M., 2000, Blueschist-bearing metamorphic core complexes in the Qiangtang block reveal deep crustal structure of northern Tibet: *Geology*, v. 28, p. 19–22, doi: 10.1130/0091-7613(2000)28<19:BMCCIT>2.0.CO;2.
- Kapp, P., Yin, A., Manning, C.E., Harrison, T.M., Taylor, M.H., and Ding, L., 2003, Tectonic evolution of the early Mesozoic blueschist-bearing Qiangtang metamorphic belt, central Tibet: *Tectonics*, v. 22, no. 4, p. 1043, doi: 10.1029/2002TC001383.
- Kong, X., Yin, A., and Harrison, T.M., 1997, Evaluating the role of pre-existing weakness and topographic distributions in the Indo-Asian collision by use of a thin-shell numerical model: *Geology*, v. 25, p. 527–530, doi: 10.1130/0091-7613(1997)025<0527:ETROPW>2.3.CO;2.
- Li, C.Y., Liu, Y., Zhu, B.C., Feng, Y.M., and Wu, H.C., 1978, Structural evolution of Qiling and Qilian Shan, in *Scientific papers in geology and international exchange*: Beijing, Geologic Publishing House, p. 174–197 (in Chinese).
- Li, S.L., Mooney, W.D., and Fan, J.C., 2006, Crustal structure of mainland China from deep seismic sounding data: *Tectonophysics*, v. 420, p. 239–252, doi: 10.1016/j.tecto.2006.01.026.
- Li, Y.H., Wu, Q.J., An, Z.H., Tian, X.B., Zeng, R.S., Zhang, R.Q., and Li, H.G., 2006, The Poisson ratio and crustal structure across the NE Tibetan Plateau determined from receiver functions: *Chinese Journal of Geophysics, Chinese Edition*, v. 49, p. 1359–1368.
- Liu, Z.Q., 1988, Geologic map of the Qinghai-Xizang Plateau and its neighboring regions (scale at 1:1,500,000): Beijing, Chengdu Institute of Geology and Mineral Resources, Geologic Publishing House.
- Métivier, F., Gaudemer, Y., Tapponnier, P., and Meyer, B., 1998, Northeastward growth of the Tibet plateau deduced from balanced reconstruction of two depositional areas: The Qaidam and Hexi Corridor basins, China: *Tectonics*, v. 17, p. 823–842, doi: 10.1029/98TC02764.
- Meyer, B., Tapponnier, P., Bourjot, L., Métiévier, F., Gaudemer, Y., Peltzer, G., Shunmin, G., and Zhitai, C., 1998, Crustal thickening in Gansu-Qinghai, lithospheric mantle subduction, and oblique, strike-slip controlled growth of the Tibet plateau: *Geophysical Journal International*, v. 135, p. 1–47, doi: 10.1046/j.1365-246X.1998.00567.x.
- Molnar, P., and Tapponnier, P., 1975, Cenozoic tectonics of Asia: effects of a continental collision: *Science*, v. 189, p. 419–426, doi: 10.1126/science.189.4201.419.
- Molnar, P., England, P., and Martinod, J., 1993, Mantle dynamics, the uplift of the Tibetan Plateau, and the Indian monsoon: *Review of Geophysics*, v. 31, p. 357–396, doi: 10.1029/93RG02030.
- Nansheng, 2002, Tectono-thermal evolution of the Qaidam Basin, China: Evidence from Rb and apatite fission track data: *Petroleum Geoscience*, v. 8, p. 279–285.
- Neil, E.A., and Houseman, G.A., 1997, Geodynamics of the Tarim Basin and the Tian Shan in central Asia: *Tectonics*, v. 16, no. 4, p. 571–584, doi: 10.1029/97TC01413.
- Owens, T.J., and Zandt, G., 1997, Implications of crustal property variations for models of Tibetan plateau evolution: *Nature*, v. 387, p. 37–43, doi: 10.1038/387037a0.
- Price, R.A., 1981, The Cordilleran foreland thrust and fold belt in the southern Canadian Rocky Mountains, in *Coward, M.P., and McClay, K.R., eds., Thrust and nappe tectonics*: Geological Society of London Special Publication, v. 9, p. 427–448.

- Price, R.A., 1986, The Southeastern Canadian Cordillera—Thrust faulting, tectonic wedging, and delamination of the lithosphere: *Journal of Structural Geology*, v. 8, p. 239–254, doi: 10.1016/0191-8141(86)90046-5.
- Qinghai, BGMR (Qinghai Bureau of Geology and Mineral Resources), 1991, Regional geology of Qinghai Province: Beijing, Geological Publishing House.
- Rieser, A.B., Neubauer, F., Liu, Y.J., and Ge, X.H., 2005, Sandstone provenance of northwestern sectors of the intracontinental Cenozoic Qaidam basin, western China: Tectonic vs. climatic control: *Sedimentary Geology*, v. 177, p. 1–18, doi: 10.1016/j.sedgeo.2005.01.012.
- Rieser, A.B., Liu, Y.J., Genser, J., Neubauer, F., Handler, R., Friedl, G., and Ge, X.H., 2006a, $^{40}\text{Ar}/^{39}\text{Ar}$ ages of detrital white mica constrain the Cenozoic development of the intracontinental Qaidam Basin: *Geological Society of America Bulletin*, v. 118, p. 1522–1534, doi: 10.1130/B25962.1.
- Rieser, A.B., Liu, Y.J., Genser, J., Neubauer, F., Handler, R., and Ge, X.H., 2006b, Uniform Permian $^{40}\text{Ar}/^{39}\text{Ar}$ detrital mica ages in the eastern Qaidam Basin (NW China): Where is the source?: *Terra Nova*, v. 18, p. 79–87, doi: 10.1111/j.1365-3121.2005.00666.x.
- Ritts, B.D., and Biffi, U., 2000, Magnitude of post-Middle Jurassic (Bajocian) displacement on the central Altyn Tagh fault system, northwest China: *Geological Society of America Bulletin*, v. 112 (1), p. 61–74.
- Royden, L.H., 1996, Coupling and decoupling of crust and mantle in convergent orogens: Implications for strain partitioning in the crust: *Journal of Geophysical Research*, v. 101, p. 17,679–17,705, doi: 10.1029/96JB00951.
- Sobel, E.R., 1999, Basin analysis of the Jurassic-Lower Cretaceous southwest Tarim basin, NW China: *Geological Society of America Bulletin*, v. 111, p. 709–724, doi: 10.1130/0016-7606(1999)111<0709:BAOTJL>2.3.CO;2.
- Sobel, E.R., Hillel, G.E., and Strecker, M.R., 2003, Formation of internally drained contractional basins by aridity-limited bedrock incision: *Journal of Geophysical Research*, v. 108, p. 2344, doi: 10.1029/2002JB001883.
- Song, S.G., Zhang, L.F., Niu, Y.L., Su, L., Jian, P., and Liu, D.Y., 2005, Geochronology of diamond-bearing zircons from garnet peridotite in the North Qaidam UHPM belt, Northern Tibetan Plateau: A record of complex histories from oceanic lithosphere subduction to continental collision: *Earth and Planetary Science Letters*, v. 234, no. 1–2, p. 99–118, doi: 10.1016/j.epsl.2005.02.036.
- Song, T., and Wang, X., 1993, Structural styles and stratigraphic patterns of syndepositional faults in a contractional setting: examples from Qaidam basin, northwestern China: *American Association of Petroleum Geologists Bulletin*, v. 77, p. 102–117.
- Sun, D.Q., and Sun, Q.Y., 1959, Petroleum potential of the Qaidam basin as viewed from the style and pattern of its structural geology: *Journal of Geomechanics*, v. 1, p. 46–57 (in Chinese).
- Sun, Z.C., Feng, X.J., Li, D.M., Yang, F., Qu, Y.H., and Wang, H.J., 1999, Cenozoic ostracoda and palaeoenvironments of the northeastern Tarim Basin, western China: *Palaeogeography, Palaeoclimatology, Palaeoecology*, v. 148 (1–3): 37–50, doi: 10.1016/S0031-0182(98)00174-6.
- Sun, Z.M., Yang, Z.Y., Pei, J.L., Ge, X.H., Wang, X.S., Yang, T.S., Li, W.M., and Yuan, S.H., 2005, Magnetostratigraphy of Paleogene sediments from northern Qaidam basin, China: Implications for tectonic uplift and block rotation in northern Tibetan plateau: *Earth and Planetary Science Letters*, v. 237, p. 635–646, doi: 10.1016/j.epsl.2005.07.007.
- Sun, Z.M., Yang, Z.Y., Pei, J.L., Yang, T.S., and Wang, X.S., 2006, New Early Cretaceous paleomagnetic data from volcanic and red beds of the eastern Qaidam Block and its implications for tectonics of Central Asia: *Earth and Planetary Science Letters*, v. 243, p. 268–281, doi: 10.1016/j.epsl.2005.12.016.
- Suppe, J., 1983, Geometry and kinematics of fault-bend folding: *American Journal of Science*, v. 283, p. 684–721.
- Suppe, J., and Medwedeff, D.A., 1990, Geometry and kinematics of fault-propagation folding: *Eclogae Geologicae Helveticae*, v. 83, p. 409–454.
- Tapponnier, P., Peltzer, G., Le Dain, A.Y., Armijo, R., and Cobbold, P., 1982, Propagating extrusion tectonics in Asia: New insights from simple experiments with plasticine: *Geology*, v. 10, p. 611–616, doi: 10.1130/0091-7613(1982)10<611:PETIAN>2.0.CO;2.
- Tapponnier, P., Meyer, B., Avouac, J.P., Peltzer, G., Gaudemer, Y., et al., 1990, Oblique thrusting and folding in the Qilian Shan, and decoupling between upper crust and mantle in northeastern Tibet: *Earth and Planetary Science Letters*, v. 97, p. 382–403, doi: 10.1016/0012-821X(90)90053-Z.
- Tapponnier, P., Xu, Z.Q., Roger, F., Meyer, B., Arnaud, N., Wittlinger, G., and Yang, J.S., 2001, Oblique stepwise rise and growth of the Tibet plateau: *Science*, v. 294, p. 1671–1677, doi: 10.1126/science.105978.
- Taylor, M., Yin, A., Ryerson, F.J., Kapp, P., and Ding, L., 2003, Conjugate strike-slip faulting along the Bangong-Nujiang suture zone accommodates coeval east-west extension and north-south shortening in the interior of the Tibetan Plateau, *Tectonics*, v. 22, 1044, doi: 10.1029/2002TC001361.
- Vincent, S.J., and Allen, M.B., 1999, Evolution of the Minle and Chaoshui Basins, China: Implications for Mesozoic strike-slip basin formation in Central Asia: *Geological Society of America Bulletin*, v. 111, p. 725–742, doi: 10.1130/0016-7606(1999)111<0725:EOTMAC>2.3.CO;2.
- Wang, E., 1997, Displacement and timing along the northern strand of the Altyn Tagh fault zone, northern Tibet: *Earth and Planetary Science Letters*, v. 150, p. 55–64, doi: 10.1016/S0012-821X(97)00085-X.
- Wang, E., Xu, F.Y., Zhou, J.X., Wan, J.L., and Burchfiel, B.C., 2006, Eastward migration of the Qaidam basin and its implications for Cenozoic evolution of the Altyn Tagh fault and associated river systems: *Geological Society of America Bulletin*, v. 118, p. 349–365, doi: 10.1130/B25778.1.
- Wang, Q., and Coward, M.P., 1990, The Chaidam Basin (NW China): Formation and hydrocarbon potential: *Journal of Petroleum Geology*, v. 13, p. 93–112.
- Xia, W., Zhang, N., Yuan, X., Fan, L., and Zhang, B., 2001, Cenozoic Qaidam basin, China: A stronger tectonic inverted, extensional rifted basin: *American Association of Petroleum Geologists Bulletin*, v. 85, p. 715–736.
- Yang, F., 1988, Distribution of the brackish-salt water ostracod in northwestern Qinghai Plateau and its geological significance, in Hanai, T., Ikeya, T., and Ishizaki, eds., *Evolutionary biology of ostracoda*: Shizuoka, Japan, Proceedings of 9th International Symposium on Ostracoda, p. 519–530.
- Yang, F., Ma, Z., Xu, T., and Ye, S., 1992, A Tertiary paleomagnetic stratigraphic profile in Qaidam basin: *Acta Petrologica Sinica*, v. 13, p. 97–101 (in Chinese).
- Yang, F., Sun, Z., Cao, C., Ma, Z., and Zhang, Y., 1997, Quaternary fossil ostracod zones and magnetostratigraphic profile in the Qaidam basin: *Acta Micropalaeontologica Sinica*, v. 14, p. 378–390 (in Chinese).
- Yang, J.S., Xu, Z., Zhang, J., Chu, C.Y., Zhang, R., and Liou, J.G., 2001, Tectonic significance of early Paleozoic high-pressure rocks in Altun-Qaidam-Qilian Mountains, northwest China, in Hendric, M.S., and Davis, G.A., eds., *Paleozoic and Mesozoic tectonic evolution of central Asia: From continental assembly to intracontinental deformation*: Boulder, Colorado, Geological Society of America Memoir 194, p. 151–170.
- Yin, A., and Harrison, T.M., 2000, Geologic evolution of the Himalayan-Tibetan orogen: *Annual Review of Earth and Planetary Sciences*, v. 28, p. 211–280.
- Yin, A., and Kelly, T.K., 1991, Structural evolution of the Lewis thrust system, southern Glacier National Park: Implications for the regional tectonic development: *Geological Society of America Bulletin*, v. 103, p. 1073–1089, doi: 10.1130/0016-7606(1991)103<1073:SEOTLP>2.3.CO;2.
- Yin, A., and Nie, S., 1996, A Phanerozoic palinspastic reconstruction of China and its neighboring regions, in Yin, A., and Harrison, T.M., eds., *The tectonics of Asia*: New York, Cambridge University Press, p. 442–485.
- Yin, A., Rumelhart, P.E., Cowgill, E., Butler, R., Harrison, T.M., Ingersoll, R.V., Cooper, K., Zhang, Q., and Wang, X.-F., 2002, Tectonic history of the Altyn Tagh fault in northern Tibet inferred from Cenozoic sedimentation: *Geological Society of America Bulletin*, v. 114, p. 1257–1295, doi: 10.1130/0016-7606(2002)114<1257:THOTAT>2.0.CO;2.
- Yin, A., McRivette, M.W., Burgess, W.P., Zhang, M., and Chen, X., 2007, Cenozoic tectonic evolution of Qaidam basin and its surrounding regions (part 2): Wedge tectonics in southern Qaidam basin and the Eastern Kunlun Range, in Sears, J.W., Harms, T.A., and Evenchick, C.A., eds., *Whence the mountains? Inquiries into the evolution of orogenic systems: A volume in honor of Raymond A. Price*: Geological Society of America Special Paper 433, p. 369–390, doi: 10.1130/2007.2433(18).
- Yin, A., Dang, Y.Q., Chen, X.H., Wang, L.C., Jiang, W.M., Zhou, S.P., and McRivette, M.W., 2008a, Cenozoic evolution of Qaidam Basin and its surrounding regions (Part 3): Structural geology, sedimentation, and tectonic reconstruction: *Geological Society of America Bulletin*.
- Yin, A., Manning, C.E., Lovera, O., Menold, C., Chen, X., and Gehrels, G.E., 2008b, Early Paleozoic tectonic and thermomechanical evolution of ultrahigh-pressure (UHP) metamorphic rocks in the northern Tibetan Plateau of NW China: *International Geology Review*, v. 49, p. 681–716.
- Zhang, J.X., Yang, J.S., Mattinson, C.G., Xu, Z.Q., Meng, F.C., and Shi, R.D., 2005, Two contrasting eclogite cooling histories, North Qaidam HP/UHP terrane, western China: Petrological and isotopic constraints: *Lithos*, v. 84, p. 51–76, doi: 10.1016/j.lithos.2005.02.002.
- Zhang, Y.C., 1997, Prototype of analysis of Petroliferous basins in China: Nanjing, Nanjing University Press, 434 p.
- Zhao, J.M., Mooney, W.D., Zhang, X.K., Li, Z.C., Jin, Z.J., and Okaya, N., 2006, Crustal structure across the Altyn Tagh Range at the northern margin of the Tibetan plateau and tectonic implications: *Earth and Planetary Science Letters*, v. 241, p. 804–814, doi: 10.1016/j.epsl.2005.11.003.
- Zhao, W.L., and Morgan, W.J., 1985, Uplift of Tibetan plateau: *Tectonics*, v. 4, p. 359–369.
- Zhao, W.L., and Morgan, W.J., 1987, Injection of Indian crust into Tibetan lower crust: A two-dimensional finite element model study: *Tectonics*, v. 6, p. 489–504.
- Zhou, J.X., Xu, F.Y., Wang, T.C., Cao, A.F., and Yin, C.M., 2006, Cenozoic deformation history of the Qaidam Basin, NW China: Results from cross-section restoration and implications for Qinghai-Tibet Plateau tectonics: *Earth and Planetary Science Letters*, v. 243, p. 195–210, doi: 10.1016/j.epsl.2005.11.033.
- Zhu, L.P., and Helmberger, D.V., 1998, Moho offset across the northern margin of the Tibetan Plateau: *Science*, v. 281, p. 1170–1172, doi: 10.1126/science.281.5380.1170.

MANUSCRIPT RECEIVED 17 JANUARY 2007
 REVISED MANUSCRIPT RECEIVED 11 AUGUST 2007
 MANUSCRIPT ACCEPTED 14 AUGUST 2007

Printed in the USA